Professur für Hydrologie

der Albert-Ludwigs-Universität Freiburg i. Br.

Anneke Ewert

Assessing SPI candidate distributions for the tropical climates of Central America

Referent: Prof. Dr. Kerstin Stahl

Korreferent: Prof. Dr. Iris Stewart-Frey

Masterarbeit unter Leitung von Prof. Dr. Kerstin Stahl

Freiburg i. Br., Oktober 2020

Table of contents

I List of figures

II List of tables

III List of figures Supplement

IV List of abbreviations

A-D test	Anderson-Darling test
Af	Tropical Rainforest
AIC	Akaike Information Criterion
Am	Tropical Monsoon
AUD	Area under drought (SPI < 1.5) [%]
Aw	Tropical Savannah
B	Arid
Cf	Temperate without dry season
CHIRPS	Climate Hazards Group Infra-Red Precipitation with Station
CHIRTS	Climate Hazards Group Infra-Red Temperature with Station
Csw	Temperate summer or winter drought
K-S test	Kolmogorov-Smirnov test
PDF	probability distribution function
SPI	Standardization precipitation index
S-W test	Shapiro-Wilk test

V Abstract

The risk of increasingly frequent and intense droughts threatens water and food security, especially for developing regions such as Central America. Central America is classified as a tropical region (A) by Köppen and Geiger, but there are regional and local differences regarding the climate. According to Köppen-Geiger's definition, there are three tropical climate classes, Af - rainforest, Am - monsoon and Aw savannah, as well as aride (B) and temperate (C) climates. This work aims to compare the different tropical climates with respect to drought. With the Standard Precipitation Index (SPI) the severity, duration and spatial extent of droughts in regions with different climates and hydrological regimes can be compared. The SPI is calculated with a parametric probability distribution function (PDF), which can lead to over- or underestimated SPI values depending on the choice of the PDF. The A-D test, S-W test and AIC were used to analyze which two-parametric distribution function is best suited for each (tropical) climate zone and accumulation period. The Gamma, Gumbel, Lognormal, Logistic, Normal and Weibull distributions as well as the accumulation periods 1, 3, 6, 9, 12 and 24 months were used. Precipitation data from the CHIRPS dataset in 0.25° spatial resolution were used for the time series from 1980 to 2019. The considered area is the land mass in the range of 25° North to 0° North and 95° West to 75° West. The results show on the one hand a difference between the accumulation periods 1 to 12 months and the very long accumulation period 24 months. On the other hand, they demonstrate a difference between the dry and rainy season of the seasonal climate zones Aw, Am and Csw. Thus, the Gamma distribution is suggested all year round for the non-seasonal climate zones Af, B and Csw and in the wet season of the seasonal climate zones Aw, Am and Csw of accumulation period 1 month to 12 months. For the very long accumulation periods (24 months) it is recommended to calculate the SPI with the most appropriate distribution for each grid cell. The Lognormal distribution is recommended for all accumulation periods in the dry period of seasonal climates.

Keywords: Drought, Central America, Climate zones, SPI, probability distribution

VI Zusammenfassung

Das Risiko zunehmend häufiger und intensiver Dürreperioden bedroht die Wasser- und Ernährungssicherheit, insbesondere für Entwicklungsregionen wie Zentralamerika. Zentralamerika wird nach Köppen und Geiger als tropische Region (A) eingestuft, jedoch gibt es regionale und lokale Unterschiede in Bezug auf das Klima. Drei tropische Klimaklassen Af – Regenwald, Am - Monsoon und Aw – Savanne sowie aride (B) und temperierte Klimata (C) sind nach der Definition von Köppen-Geiger vertreten. Ziel dieser Arbeit ist, die verschiedenen tropischen Klimazonen in Hinblick auf Dürre zu vergleichen. Mit dem Standardniederschlagsindex (SPI) können Intensität, Dauer und räumliche Ausdehnung von Dürren in Regionen mit unterschiedlichen Klimata und hydrologischen Regimen verglichen werden. Der SPI wird mit einer parametrischen Wahrscheinlichkeitsfunktion berechnet, welche je nach Wahl zu über- oder unterschätzen SPI-Werten führen kann. Dazu wurde anhand von A-D Test, S-W Test und AIC analysiert, welche zwei-parametrische Verteilungsfunktion am besten für die jeweilige (tropische) Klimazone und Akkumulationsperiode geeignet ist. Verwendet wurden Gamma, Gumbel, Lognormal, Logistic, Normal und Weibull Verteilung sowie die Akkumulationsperioden 1, 3, 6, 9, 12 und 24 Monate. Hierfür wurden Niederschlagsdaten aus dem CHIRPS-Datensatz in 0,25° räumliche Auflösung für die Zeitreihe von 1980 bis 2019 verwendet. Das betrachtete Gebiet ist die Landmasse im Bereich von 25° Nord bis 0° Nord und 95° West bis 75°West. Die Ergebnisse zeigen einerseits einen Unterschied zwischen den Akkumulationsperioden 1 bis 12 Monate und der sehr langen Akkumulationsperiode 24 Monate. Andererseits weisen sie einen Unterschied zwischen Trocken- und Regensaison der saisonalen Klimazonen Aw, Am und Csw auf. Folglich kann ganzjährig für die nicht saisonalen Klimazonen Af, B und Csw und in der Regenzeit der saisonalen Klimazonen Aw, Am und Csw von Akkumulationsperiode 1 Monat bis 12 Monate die Gamma Verteilung empfohlen werden. Für sehr lange Akkumulationsperioden (24 Monate) wird empfohlen, den SPI mit der für jedes Grid am besten passenden Verteilung zu berechnen. Die Lognormalverteilung wird für alle Akkumulationsperioden in der Trockenperiode der saisonalen Klimazonen empfohlen.

Stichwörter: Dürre, Zentralamerika, Klimazonen, SPI, Wahrscheinlichkeitsverteilungen

1. Introduction

1.1 Current situation and definition of drought

Changes in the Earth's climate have led to changes in the frequency and intensity of various hydrometeorological processes such as precipitation, temperature, evaporation and runoff (Crausbay et al., 2017; Liu et al., 2019). With the increasing concentrations of greenhouse gases in the atmosphere, the precipitation-related risks of climate change will almost certainly grow (Touma et al., 2015). Future climate scenarios indicate general warming and lower precipitation trends (Imbach et al. 2018, van Oldenborgh et al. 2013) with increased extremes (Nakaegawa et al, 2014). The intensification of human activities, including urbanization, deforestation, construction of water reservoirs, contributes to an accumulation of drought events (Trenberth et al. 2014). Drought can be defined as a lack of water over a long period of time or as a quantity of water that is below average in the inspected water circulation system during a certain period (Khan et al., 2018; Oloruntade et al., 2017). It is one of the most frequent and costly natural disasters, with immense impacts on human society and ecosystems (Mishra & Singh 2010; Wilhite 2000).

There are three types of drought (Keyantash and Dracup, 2002; Mishra and Singh, 2010): (1) Meteorological drought, a precipitation deficit compared to the average values over a certain period. (2) Hydrological drought, characterized by an insufficient water supply compared to established water uses and management approaches, often related to the geology of the basin. (3) Agricultural drought characterized by a period of insufficient soil moisture and associated crop failures. Some publications also define a fourth category: (4) Socio-economic drought, the inability to meet the water needs of a concerned society (e.g. Choi et al., 2013; Heim & Brewer, 2012). Drought is triggered by below-average rainfall, typically accompanied by high summer temperatures (Diffenbaugh et al. 2015; Diego Galván et al. 2015). The duration, intensity, spatial extent and local socio-economic conditions determine the severity of droughts (Wilhite, 2000). In the future, periods of drought will become more frequent, more intense, longer and therefore more severe (Touma et al., 2015). As a result, drought is an important planning criterion for the sustainable management of water resources (Crausbay et al., 2017; Liu et al., 2019). Droughts can also result in humanitarian disasters, major agricultural as well as economic losses and harm ecosystems (Lesk et al., 2016; Touma et al., 2015; Van Loon et al., 2016). Therefore, the identification of drought-prone areas and the prediction of drought periods are of immense interest for research and from a political point of view. The detected results can help to respond to drought events and reduce socio-economic costs (Mishra & Singh 2011).

1.2 Study area and local drought on site

The growing risk of increasingly frequent and more intense droughts threatens water and food security, especially for developing regions such as Central America. This area includes southern Mexico, Guatemala, Belize, El Salvador, Honduras, Nicaragua, Costa Rica, Panama and a part of north Columbia. Central America is an isthmus bridge between two continents, bordering the Pacific Ocean in the southwest as well as the Caribbean Sea in the northeast (Figure 1). In a few kilometers of horizontal distance, the complex topography varies from volcanic peaks of about 4000 m above sea level, jungle-covered alluvial lowlands and rugged coastlines to lagoons (Imbach et al., 2018, Marshall, 2007). Honduras ranks first in the long-term climate risk index, Nicaragua and Guatemala are listed in the top ten (Kreft et al., 2017). Those states are already suffering from the effects of climate change as a result of historical warming (Aguilar et al., 2005). Vulnerability to climate extremes is high due to the economy's strong dependence on agriculture and hydropower. Small farmers are a particularly vulnerable group in the happening of extreme climate changes (Imbach et al.2017).

Figure 1: Central America topography with republics with their capitals (https://www.britannica.com/place/Central-America)

Central America is classified as a tropical region (A) according to Köppen and Geiger. However, there are regional and local differences in climate, all three tropical climate classes are represented: Af - rainforest, Am - monsoon and Aw – savannah (Beck et al. 2018). Due to the tropical-maritime location, the temperature fluctuations in the entire region are low. Temperature is mainly influenced by altitude and distance from the oceans. In general, it decreases with enlarging altitude and increases with distance from the coast (Clawson, 1997). The warmest months generally occur at the end of the wet season in October. Precipitation is the most important meteorological element (Taylor and Alfaro, 2005). Central America has a rainy season from May to October (Hastenrath, 1967), which is characterized by two precipitation maxima in May/June and September/October. Both of them are essential for the planting and harvesting cycle (Bacon et al., 2017; Magaña et al., 1999). In the dry corridor of Central America, they are separated by a period with less precipitation, the "Mid-Summer-Dry"

(Avelino et al., 2015). The extended dry season is between November and May. On the Caribbean coasts it rains all year round, the most from October to December and the least between January and April (Magaña et al., 1999). Due to north-eastern trade winds, the annual precipitation sum decreases from east to west (Martinson, 1993), the Caribbean side receives between 4000 and 6500 mm of precipitation per year, while the Pacific coastal areas receive less than 1500 mm of precipitation per year (Bundschuh et al., 2007). Due to climate change, precipitation in Central America will generally decrease and the entire region is expected to warm, especially in the northern part (Imbach et al. 2018). The severity and frequency of droughts in subtropical and tropical areas are increasing (Touma et al., 2015). The midsummer drought may spread to regions that have not been affected in the past. In regions, in which it already occurs in the presence, its severity may increase in the future (Imbach et al. 2018). Shifts in the rainy season or a longer, more extreme Mid-Summer-Dry-period increase the probability of crop failures, pest outbreaks and plant diseases (Avelino et al., 2015). In the past 20 years, severe droughts affected large parts of Central America simultaneously, one in the year 2001 (Ramirez and Brenes, 2001) and another one 2014, from April to August (Chen et al. 2017). The drought in 2014 was the heaviest since 2001 (Chen et al, 2017).

The countries of Central America, except for Mexico, are relatively small in population, area, and size of economies (Acosta et al., 2017). Including total Mexico, overall population was 177.6 million in 2016 with an annual population increase of about 1.2 % (United Nations, 2019). Central America has got the highest poverty rates in Latin America, about 42 % of the region's population is poor or extremely poor (Krozer, 2010). The largest part of the regional economy is based on agriculture, more than two thirds of the population in Guatemala, Honduras and Nicaragua are dependent on it (Imbach et al., 2018). The most important export product in Central America is Coffee with a value of $3.70B in 2011, followed by bananas ($1.64B), sugar ($1.03B) and palm oil ($0.68B) (FAO, 2012). Food security mainly depends on maize, rice and beans (Espíndola et al. 2005). Nicaragua is highly vulnerable to climate change (Bouroncle et al., 2017) especially for coffee (Läderach et al., 2017), maize and bean (Gourdji et al., 2015). The predicted losses in coffee production threaten national economies and the regional and global supply chains of the respective industries (Bunn et al., 2015). Food security can also be affected by interruptions in production. Furthermore, food security could be harmed by disturbances in the production of e.g. corn and beans. The supply of drinking water becomes more expensive due to reduced water levels in surface and underground water bodies, which leads to increased costs of water abstraction; alternative ways of drinking water supply may be necessary (Brenes, 2010).

1.3 Drought monitoring with SPI

Various indices have been developed to quantify the severity of drought, which have been applied to different regions and conditions (e.g. Keyantash and Dracup, 2002, Quesada Montano et al., 2015; Vicente-Serrano et al., 2010). Recommended by the World Metrologic Organization as a meteorological drought index is the well-reviewed and globally applied standardization precipitation index (SPI) (Hayes et al., 2011). SPI values represent the deviation from the typical cumulative precipitation over the months under consideration for a specific location and season (McKee et al., 1993). Variable time scales allow the evaluation of meteorological drought with short accumulation times e.g. 1 to 3 months, agricultural drought with medium accumulation times e.g. 3 to 6 months and hydrological drought with long accumulation times e.g. 6 to 12 months (Lloyd-Hughes and Saunders, 2002). The fundamental strength of the SPI is that it can be calculated for a variety of time scales and is based on precipitation only. This makes it particularly suitable for regions with limited data availability and for comparing drought conditions in regions with significantly different climates (McKee et al., 1993).

The SPI is based on a representative parametric probability distribution function (PDF), the choice of which can lead to exaggerated or reduced SPI values and thus to potentially incorrect estimates of the timing, intensity and duration of droughts (Guenang et al., 2019; Stagge et al., 2015). Most recent studies have analyzed only 2-parameter distribution functions (Guenang et al., 2019; Blain et al., 2018; Stagge et al., 2015; Lloyd-Hughes and Saunders, 2002), since testing the quality of 3-parameter distributions carries the risk of overfitting (Stagge et al., 2015; Sienz et al., 2012). To describe the observed precipitation best, McKee et al (1993) originally recommended a two-parameter Gamma distribution. This distribution is one of the most used today to calculate the SPI. As a result, many studies that include the SPI directly use the Gamma distribution (e.g. Mo and Lyon, 2015; Ma et al., 2015; Yuan and Wood, 2013; Yoon et al., 2012). The normality of the resulting SPI distribution is not previously evaluated by goodness-of-fit tests or other statistical analyses. Several authors, on the other hand, point out that for new datasets and regions, the distribution functions should be investigated before they are applied (Blain et al., 2018; Stage et al., 2015; Sienz et al., 2012; Touma et al., 2015). In some regions of the world, the adjusted Gamma distribution function describes precipitation inadequately (Blain et al., 2018; Blain and Meschiatti, 2015; Guenang et al., 2019; Lloyd-Hughes and Saunders, 2002; Naresh Kumar et al., 2009; Stage et al., 2015; Sienz et al., 2012; Touma et al., 2015).

Stagge et al. (2015) have developed a methodology to determine the most appropriate probability functions in a geographical region. They found that the Gamma and Weibull functions have broad effectiveness across often contrasting regions of Europe. Lloyd-Hughes and Saunders (2002) have also identified Gamma distribution as the best distribution function for Europe. The results of Stagge et al (2015) were developed using the watch forcing data set and for the European geographical region but were not evaluated for other data sets or geographical regions. For SPI calculation in Central Africa, the use of the Weibull and Gamma functions leads to good SPI results on short time scales (1 to 9 months). For a 12-month time scale, it is recommended to choose the distribution function with the best fit for each grid point to obtain good SPI results and to ensure a better description of the drought (Guenang et al., 2019). Additionally, in China, the Gamma distribution scores best on almost all-time scales when calculating the SPI. However, on the 1-month scale, the Log-Logistic and Weibull distribution have a higher percentage of the best relative fit than the Gamma distribution (Wang et al., 2019). Along with three goodness-of-fit tests, it was determined that the two-parameter Gamma distribution among the two-parameter functions is the most appropriate distribution for calculating the SPI in the State of São Paulo, Brazil (Blain et al., 2018). The same conclusion is drawn by other studies such as Meschiatti and Blain (2016) and Awange et al. (2016), who also used the Gamma distribution to calculate the SPI in São Paulo State. All these studies agree that either the Weibull or Gamma distribution is the most appropriate, depending on the accumulation period and/or location. The candidate probability density functions worldwide were tested by Touma et al (2015) and Pieper et al (2020). Touma et al (2015) deal only globally with accumulation periods between 3 and 12 months and conclude that the Gamma distribution is best suited to calculate the SPI. Pieper et al. (2020) also show that the Gamma distribution is sufficiently suitable to calculate the SPI.

In most studies, candidate distribution functions are tested with the goodness of fit tests (Guenang et al., 2019; Blain et al., 2018; Blain and Meschiatti, 2015; Stagge et al., 2015; Touma et al., 2015; Lloyd-Hughes and Saunders, 2002). The Kolmogorov-Smirnov test (K-S test) is often used (Guenang et al., 2019; Touma et al., 2015), but it has a high probability of erroneously accepting a non-normal distribution if the parameters of the PDF candidate were estimated from the same data on which the tested distribution is based (Blain et al., 2018; Blain and Meshiatti, 2015; Stage et al., 2015). It also proved to be the least sensitive to proposed distributions (Stagge et al., 2015). Therefore, the goodness of fit has been tested in other studies either with an adaptation of the K-S test, the Anderson-Darling test (A-D test) (Blain et al., 2018; Stage et al., 2015) and/or with the Shapiro-Wilk test (S-W test) (Blain et al., 2018; Blain

and Meshiatti, 2015; Stage et al., 2015). The Anderson-Darling test is inferior to the Shapiro-Wilk test and gives more weight to the tails than does the K-S test (Blain et al., 2018; Stagge et al., 2015). The S-W test for testing the normality of the calculated drought index effectively differentiates between candidate distributions and provides similar results to the K-S and A-D tests with more sensitive results. It is also easy and quick to implement, eliminating the need for Monte Carlo simulations of critical test values. Spatial patterns similar to the relative rankings calculated by AIC are generated (Stagge et al., 2015). Nevertheless, the Shapiro-Wilk test is unreliable to assess SPI normality (Naresh Kumar et al., 2009). K-S, A-D and S-W test are unable to produce a relative ranking of the performance of the distribution functions for a given location and accumulation period and therefore are unsuitable for determining the best performing PDF (Blain et al., 2018). This is because these suitability tests are designed to provide a binary response (Blain et al., 2018). The goodness-of-fit tests are well suited to analyze whether SPI distributions are normally distributed, but it’s more important which PDF maximizes the normality of the resulting SPI distribution. The use of relative ratings such as mean absolute errors (Blain et al., 2018), Akaike's Information Criterion (AIC) (Stagge et al., 2015; Sienz et al., 2012) or deviations from expected SPI categories (Sienz et al., 2012) is recommended instead.

1.4 Problem and objective

SPI studies covered both North and South America (Blain et al., 2018; Pieper et al., 2020), but not Central America, and there is no study on this region yet. This study attempts to close the knowledge gap regarding Central America. Previous studies examine the best performance of the PDF only over the respective overall area considered. In contrast, I will divide Central America into its climate zones by Köppen and Geiger to analyze whether the climate regime is decisive for the best performing PDF. Drought is mainly influenced by precipitation and temperature (Diffenbaugh et al. 2015; Diego Galván et al. 2015), which are also the criteria for climate zones according to Köppen and Geiger (Köppen, 1936). A correlation between drought indices such as the SPI and climate zones might therefore be possible. To analyze the best performing PDF I will use the Anderson-Darling test, the Shapiro-Wilk test and the AIC for comparing the results. I focus on the SPI accumulation periods of 1, 3, 6, 9, 12 and 24-months and test the performance of the Gamma, Gumbe l, Lognormal, Logistic, Normal and Weibull function.

The aim of this thesis is to analyse the best performing PDF for the different (tropical) climate zones in Central America using the following hypotheses:

I. To derive the SPI, the Gamma (accumulation period ≥ 3) and Weibull distribution (accumulation period < 3) functions shows the best performance for each of the tropical climate zones in Central America.
II. There are no seasonal differences in the adjustment of candidate distributions for the SPI for different accumulation periods in the Central American climate zones.
III. Various distributions estimate the area under drought (SPI < 1.5) differently compared to the best fit (for each grid cell, the best fit distribution is used to calculate the SPI).

2. Data and methods

2.1 Overall structure and datasets

First, the climate zone according to Köppen and Geiger was calculated for each grid (0.25°x0.25°). For the following evaluations, all grids of a climate zone were considered as one, whereby the arid climates were combined to a climate zone and the temperate zones were divided into seasonal and non-seasonal. Then the SPI was calculated with the distribution functions Gamma, Gumbel, Normal, Lognormal, Logistic and Weibull. The accumulation periods of 1, 3, 6, 9, 12 and 24 months were used. The calculation outputs two parameters for each distribution with the accumulation period. With this parameter, the Anderson-Darling rejection rate is calculated for the goodness of fit. As a further goodness of fit test, the Shapiro and Wilk test, which examines the SPI values directly was used. To illustrate the best relative fit the AIC was calculated.

The area focused on is Central America in the range of 25° North to 0° North and 95° West to 75° West. The quality and quantity of the data used determines the reliability of the drought characterization. Quesada Montano (2019) recommends to supplement station data with CRN073 and/or CHIRPS for the characterization of droughts in Central America. All analyses are performed with the Climate Hazards Group Infra-Red Precipitation with Station (CHIRPS) dataset, an over 30 years quasi-global gridded rainfall dataset, starting in 1981 through the near-present (Funk et al., 2015). CHIRPS uses satellite imagery at the 0.05° spatial resolution and in-situ station data to generate a daily climate dataset (Funk et al., 2015). For this work precipitation data from the CHIRPS dataset in 0.25° spatial resolution for the monthly time series from 1980 to 2019 are used.

There is also temperature data needed for the climate classification. Therefore, I used a CHIRTS dataset from 1983 to 2016 in 0.25° spatial resolution. The data is either available on a monthly or a daily base. In this case, the monthly data collection was used.

Divide Central America into climate classes

Calculated with the Köppen and Geiger classification for each Grid

Climate zones for evaluation: Am, Aw, Af, arid climates were combined to B and the temperate zones were divided into seasonal Csw and non-seasonal Cf

Size structure:

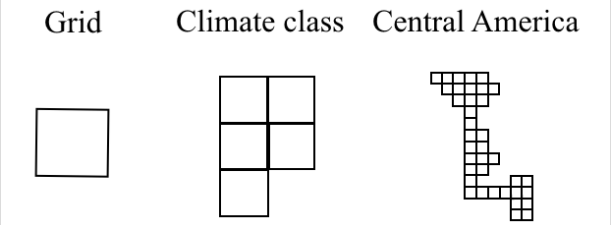

SPI calculation with different distribuion functions

Distribution functions: Gamma, Gumbel, Normal, Lognormal, Logistic and Weibull
Accumulation periods: 1, 3, 6, 9, 12 and 24 month

SPI calculation outputs two parameters per distribution function and month (January to December)

Goodness of Fit for each climate class

Rejection Frequency for Anderson-Darling and Shapiro and Wilk test with the output from SPI calculation

- In total for the climate zones
- Per Month and climate zone

Best relative fit with AIC:

- Dry season (January, February, March)
- wet season (July, August, September)

Implementation on drought period 2014/2015

SPI on July 2014

- Gamma, Logistic, Lognormal and best fit (according to AIC) distribution
- Accumulation period 1, 6 and 12 months

Area under drought from january 2014 to december 2015

- Gamma, Logistic, Lognormal and best fit (according to AIC) distribution
- Accumulation period 1, 6 and 12 months

Difference between Area under drought best fit and Gamma/Logistic/Lognormal distribution from january 2014 to december 2015

- Accumulation period 1, 6 and 12 months

Figure 2: Float chart of the overall structure for evaluation

2.2 Köppen-Geiger climate classification

The Köppen-Geiger climate classification described by Peel et al. (2007) was used (Table 1). This classification is almost identical to the last publication of Köppen (1936) and as well applied by Kriticos et al (2012) and Beck et al (2018). There are two differences to Köppen (1936): Firstly, as the exception of the boundary between the temperate (C) and cold (D) climates the temperature of the coldest month >0 °C, instead of >–3 °C was used (followed Russell, 1931). Secondly, within the C and D climates, the sub-climates s (dry summer) and w (dry winter) were made exclusive for each other. These differences are not relevant for the tropical climate zones regarded in this thesis. The tropical (A), temperate (C), cold (D) and polar (E) climates are mutually exclusive, but each zone may overlap with the arid zone (B) (Beck et al., 2018). Hence, climate type B was given precedence over climates A, C, D and E. The classification was performed for the monthly CHIRPS and CHIRTS data sets with R.

Table 1: Overview of the Köppen-Geiger climate classes occurring in Central America including the defining criteria. Adapted from Peel et al. (2007). T_{cold} = the air temperature of the coldest month (°C); P_{dry} =precipitation in the driest month (mm month−1); MAP = mean annual precipitation (mm y−1), threshold = 20×MAT if >70% of precipitation falls in winter, 20×MAT+280 if >70% of precipitation falls in summer, otherwise 20×MAT+140; MAT = mean annual air temperature (°C); T_{hot} = the air temperature of the hottest month (°C); P_{sdry} = precipitation in the driest month in summer (mm month−1); P_{wdry} = precipitation in the driest month in winter (mm month−1); P_{swet} = precipitation in the wettest month in summer (mm month−1); P_{wwet} = precipitation in the wettest month in winter (mm month−1), T_{4th_hot} = temperature of the 4th warmest month (°C)

Letter symbol			**Description**	**Criterion**
A			Tropical	$T_{cold} \geq 18$
	f		- Rainforest	$P_{dry} \geq 60$
	m		- Monsoon	Not (Af) & $P_{dry} \geq 100\text{-}MAP/25$
	w		- Savannah	Not (Af) & $P_{dry} < 100\text{-}MAP/25$
B			Arid	MAP <threshold
	W		- Desert	MAP <threshold/2
	S		- Steppe	MAP ≥threshold/2
		h	- Hot	MAT ≥18
		k	- Cold	MAT <18
C			Temperate	$0 < T_{cold} < 18$ & $T_{hot} > 10$
	s		- Dry summer	$P_{sdry} < 40$ & $P_{sdry} < P_{wwet}/3$
	w		- Dry winter	$P_{wdry} < P_{swet}/10$
	f		- Without dry season	Not (Cs) and (Cw)
		a	- Hot summer	$T_{hot} \geq 22$
		b	- Warm summer	Not (a) & $T_{4th\_hot} > 10$

2.3 Standardization Precipitation Index (SPI)

2.3.1 Calculation with different candidate distribution functions

The SPI evaluates and characterizes the precipitation ratio of a certain period (e.g. month, quarter and half-year) in relation to the respective normal values. For the calculation, the precipitation is summed over k months (accumulation period). The distribution function of the precipitation values is transformed into a standard Normal distribution (μ =0, σ =1). For each precipitation value, the position specified in standard deviations can be given in the distribution function, which corresponds to the SPI value (McKee et al., 1993; Guttman, 1999; Lloyd-Hughes and Saunders, 2002). The SPI is limited to the range of [-3, 3] to obtain realistic results. The probability of leaving this range is very low (<0.2 %) (Stage et al., 2015). A negative SPI value indicates a period that was drier than normal, a positive SPI value indicates a period that was wetter than normal. A drought occurs when the precipitation value is less than minus one standard deviation. Drought intensity is arbitrarily defined for values of the SPI (**Fehler! Verweisquelle konnte nicht gefunden werden.**). An SPI of less than 1.5 is often used as a threshold for severe droughts. More detailed information can be found in McKee et al. (1993). Zero-precipitation values strongly distort the SPI results. To prevent this, the probability of zero-precipitation events (p0) was estimated by the "center of gravity" estimation based on the zero distribution. The SCI R package from Gudmundsson and Stagge (2014) is used for programming, which contains the described approach.

Table 2: The classification of SPI after McKeen et al. (1993)

SPI Values	**Drought Category**
0 to -0.99	Mild drought
-1.00 to -1.49	Moderate drought
-1.5 to -1.99	Severe drought
≤ -2.00	Extreme drought

The time scales considered for the SPI in this thesis are 1-, 3-, 6-, 9-, 12- and 24-months and the evaluated distribution function will be the (a) Gamma, (b) Gumbel, (c) Normal, (d) Lognormal, (e) Logistic and (f) Weibull distributions. Area under drought [%] is defined as surface with drought category severe and extreme drought (SPI ≤ -1.5) per climate class. All distribution functions are calculated with two parameters as defined below:

(a) Gamma distribution:

$$f\,(x) = \frac{1}{\alpha^{\beta}\Gamma\,(\beta)}x^{\beta-1}\,e^{-x/\alpha}, \qquad x\,>0 \tag{1}$$

$$\text{Where: } \Gamma\,(c)\;=\;\int_0^{\infty} e^{-x}x^{c-1}dx \tag{2}$$

(b) Gumbel distribution:

$$f\,(x) = \left(\frac{1}{\sigma}\right)e^{-z(x)-e^{-z(x)}}, \quad -\infty\,<\,x\,<\,\infty \tag{3}$$

$$\text{Where: } z\,(x)\;=\;\frac{x\,-\,\mu}{\sigma} \tag{4}$$

(c) Normal distribution:

$$f\,(x) = \frac{1}{\sigma\sqrt{2\pi}}\exp\left[-\frac{1}{2}\left(\frac{x\,-\,\mu}{\sigma}\right)^2\right], \qquad -\infty\,<\,x\,<\,\infty \tag{5}$$

(d) Lognormal distribution:

$$f\,(x)\;=\;\frac{1}{\beta x\sqrt{2\pi}}e^{\left[-\frac{1}{2}\left(\frac{log\frac{x}{\alpha}}{\beta}\right)^2\right]}, \qquad x\;>\;0 \tag{6}$$

(e) Logistic distribution:

$$f(x)\;=\;\frac{\lambda^{\kappa}\kappa e^{\kappa x}}{[1\;+\;(\lambda e^{x})^{\kappa}]^2}, \qquad -\infty\,<\,x\,<\,\infty \tag{7}$$

(f) Weibull distribution:

$$f\,(x)\;=\left(\frac{\beta}{\alpha}\right)x^{\beta-1}\,exp\left[-\left(\frac{1}{\alpha}\right)x^{\beta}\right], \qquad x\;>\;0 \tag{8}$$

2.3.2 Goodness of fit testing

The parametric probability function, with which the SPI is calculated, can lead to over- or underestimated SPI values depending on the choice. Stagge et al. (2015) developed a methodology to determine the most appropriate probability function in a geographical region. Based on Stagge et al. (2015), the performance of each probability distribution function is tested by different goodness-of-fit tests. I used the Anderson-Darling (A-D) test as well as Shapiro and Wilk (S-W) test.

The A-D statistics are used to determine how well data corresponds to a distribution. It is a modification of the Kolmogorov-Smirnov (K-S) (Stephens, 1986) test and gives more weight to the tails than the K-S test. The test statistic is:

$$A = -n - \frac{1}{n}\sum_{i=1}^{n}\sum [2i-1][ln(p_{(i)}) + ln(1 - p_{(n-i+1)})] \quad \textbf{(9)}$$

with $p_{(i)} = \Phi([x_{(i)} - \bar{x}]/s)$, Φ is the cumulative distribution function of the standard normal distribution, and $\bar{x}$ and s are mean and standard deviation of the data values (Stephens, 1986). Furthermore, the p-value is computed from the statistic:

$$Z = A(1.0 + \frac{0.75}{n} + \frac{2.25}{n^2}) \quad \textbf{(10)}$$

The corresponding p-value is used to test whether the data comes from the selected distribution. If the p-value is less than the selected alpha level (0.05), the null hypothesis that the data came from that distribution is rejected. In contrast, a p-value of more than the selected alpha level does not necessarily mean that the frequency distribution of the data corresponds to the given distribution (Stephens, 1986).

The Shapiro-Wilk test (Shapiro and Wilk, 1965) examines whether a sample is distributed normally. This method was first used for the SPI by Naresh Kumar et al. (2009). An S-W test is beneficial because it directly tests the final index values, it is independent of the PDF used and it has well verified and sensitive critical values. The test statistic is the quotient of two estimates of variance:

$$W_{pr} = \frac{b^2}{(n-1)s_x^2} \quad \textbf{(11)}$$

with expected variance of the sample under normal distribution b^2 and s_x^2 uncorrected sampling variance. The null hypothesis that there is a normal distribution of the population is not rejected

if the p-value is higher than the defined alpha level. The SW-test has a comparatively high-test strength, especially when testing smaller samples with n < 50 (Seier, 2011).

The distributions were compared relative to each other using the Akaike Information Criterion (AIC) (Akaike, 1974; Burnham and Anderson, 2004). It is a mathematical method for evaluating how well a distribution fits the data from which it was generated. But it is not a statistical test and therefore cannot provide information on the absolute goodness of fit. It determines the relative information value of the model using the log-likelihood estimate and the number of parameters. All distributions have the same number of parameters (two), which reduces the AIC to a measure of logarithmic probability. The log-likelihood is the value that describes how probable the model is regarding the data. The formula for AIC is:

$$AIC = -2LL + 2k \tag{12}$$

where k being the number of independent variables used and LL representing the log-likelihood. The distribution that contains the greatest amount of variation with the fewest independent variables shows the best fit. The lower the AIC values, the more precisely the distribution fits.

However, the A-D test is inferior to the S-W test (Blain et al., 2018), which is why the S-W test can be considered more meaningful. To determine the best performing PDF, the use of relative ratings such as the AIC instead of A-D and S-W test is recommended (Stagge et al., 2015; Sienz et al., 2012). So the best fit distribution function at each grid point, called best fit in this study, can be chosen in order to expect good SPI results.

3. Results

3.1 Climate regions in Central America

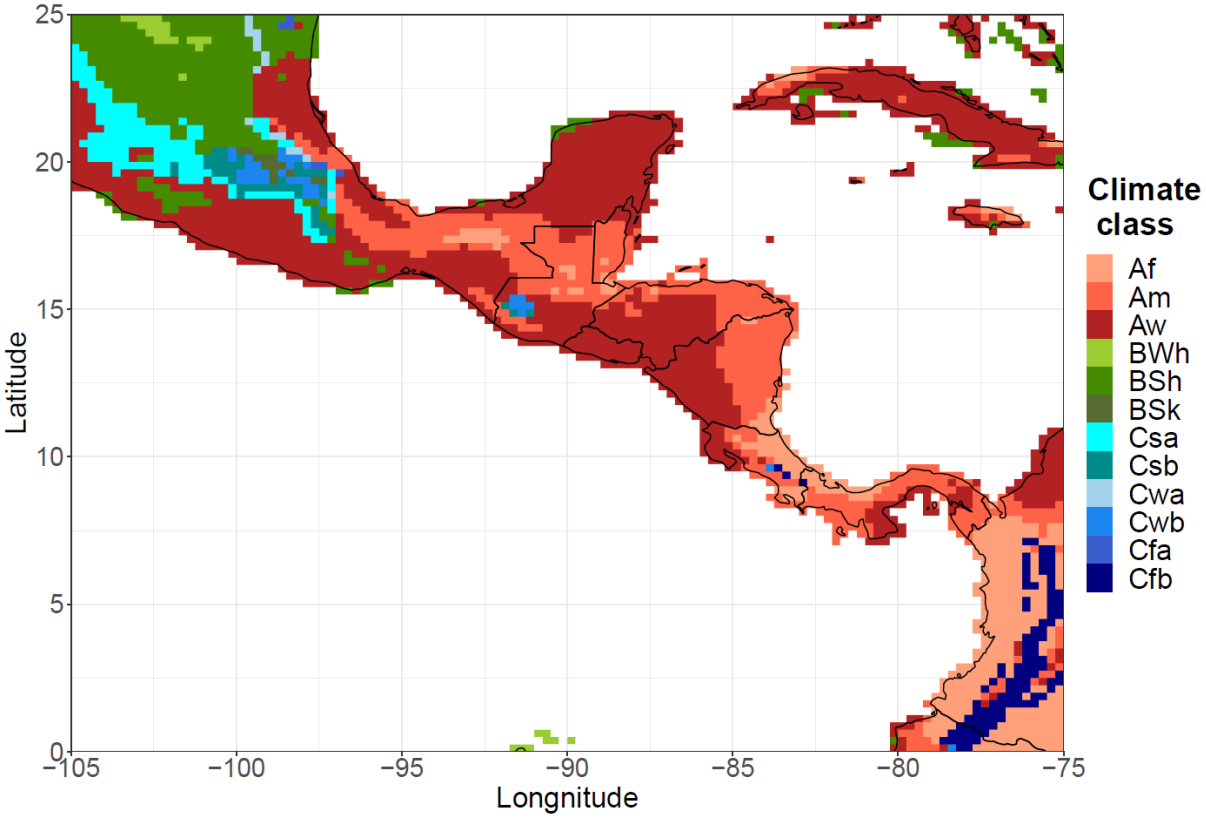

Figure 3: Köppen and Geiger climate classes after Peel et al. (2007) for Central America

About two thirds of Central America is located in the tropical climate zone (Figure 3). The tropical savannah (Aw) has the largest share with 43 %, followed by tropical monsoon (Am, 19 %) and tropical rainforest (Af, 12 %). Furthermore, arid (B, 15 %) and temperate (C, 11 %) climate zones occur in Central America. The largest climate zone outside the tropics is the hot arid steppe (BSh) with 13 % of the land mass. All other existing climate zones are below 5 % of the area. For the following evaluations, all grids of a climate zone were considered together, whereby the arid climates were combined to B and the temperate zones were divided into seasonal Csw and non-seasonal Cf.

3.2 Goodness of fit of A-D and S-W test for candidate distributions from SPI

Table 3 shows the A-D and S–W rejection frequency (α = 5%), defined as the ratio of rejected distributions across all land surface grids in Central America and 12 month-fitted distributions for each tested accumulation period. The A-D and S-W test, which are used to test the quality of fit, each form two groups with respect to normality. For the A-D test the two groups can be divided into (1) long-accumulation distributions, of which the Logistic distribution dominates, and (2) short-accumulation distributions, of which the Gumbel distribution fits best. The rejection rate of the A-D test is generally low from SPI 3. The S-W rejection rate can be classified into the groups (1) accumulation periods within one year, of which the Gamma distribution dominates, and (2) very long accumulation periods, of which the Logistic distribution fits best. For the S-W test, the Gamma distribution performs best for all accumulation periods except SPI 24, where it still has the second-best distribution with 10.0 % rejection. Both A-D and S-W test classify the Logistic distribution as most suitable for SPI 24.

Table 3: Rejection frequencies (%) for Anderson–Darling (A–D) and Shapiro–Wilk (S–W) test for all tested distributions and SPI accumulation periods over hole Central America

	SPI 1		SPI 3		SPI 6		SPI 9		SPI 12		SPI 24	
	AD	SW	AD	SW	AD	SW	AD	SW	AD	SW	AD	SW
Gamma	9.9	**21.7**	1.6	**8.2**	0.3	**6.2**	0.1	**6.7**	0.1	**7.3**	0.4	11.0
Gumbel	**3.7**	25.5	0.7	15.8	0.6	19.6	0.6	24.4	0.8	27.3	1.4	34
Logistic	4.7	52.1	**0.5**	26.2	**0.1**	12.8	**0**	8.9	**0**	8.3	**0**	**10**
Lognormal	9.6	22.5	1.8	10.3	0.5	8.1	0.4	8.2	0.4	8.3	0.6	11.7
Normal	12.7	59.6	2.4	34.3	0.4	18.5	0.3	13.1	0.2	11.6	0.4	13.2
Weibull	8.8	39.8	1.4	34.8	0.5	34.4	0.3	36.9	0.2	38.9	1.1	42.4

Figure 4 and Figure 5 show the A-D and S–W rejection frequency (α = 5%) for each climate zone, defined as the ratio of rejected distributions across all land surface grids of the corresponding climate zone and 12 month-fitted distributions for each tested accumulation period. For Am, the rejection frequency of the A-D test at SPI 1 (0.34%) and SPI 3 (0.05%) is lowest for the Gumbel distribution. From SPI 6 on, the rejection frequency is too low, therefore no difference can be seen (Figure 4a). The S-W test shows the lowest rejection frequency for the Gamma function from SPI 1 to SPI 6, while from SPI 9 to SPI 24 the Logistic distribution has the lowest rejection rate. The Gamma distribution has the second lowest rejection frequency for these accumulation periods (Figure 4b). Also, for the climate zone Aw the rejection rate of the A-D test is lowest for the Gumbel distribution at SPI 1 and SPI 3. From SPI 6 on, the rejection rates are low again, except for SPI 24, where the Weibull distribution has a relatively

high rejection rate (1.94%) (Figure 4c). The rejection rate of the S-W test at SPI 1 is lowest for the Lognormal function (23.22%), while for all other accumulation periods the Gamma distribution has the lowest rejection rate (Figure 4d). The A-D test for climate zone Af consistently shows the best goodness of fit for the Logistic function (Figure 4e). Even in the S-W test, the Logistic function has the highest goodness of fit from SPI 6 to SPI 24. Regarding SPI 1 (10.73%) and SPI 3 (8.56%), the rejection frequency of the Gamma distribution is lowest (Figure 4f).

In general, the rejection frequency grows with an increasing accumulation period for the A-D and S-W test for this climate zone. B shows the highest overall rejection frequency of the goodness of fit tests. The rejection frequency of the A-D test at SPI 1 to SPI 6 is lowest for the Gumbel distribution. From SPI 9 on, the rejection frequency is too low to see a difference (Figure 5**Figure 4**a). The S-W test consistently shows the best fitting quality for the Gamma function (Figure 5b). The A-D test for climate zone Csw shows the best goodness of fit for the Gumbel function by SPI 1 (2.87%) and SPI 3 (0.07%) (Figure 5c). Candidate distributions for SPI form two distinct groups with respect to the S–W test. These groups can be divided into (1) accumulation distributions of 9 to 24 months, of which the Logistic distribution dominates, and (2) shorter-accumulation distributions (1 to 6 month), of which the Gamma distribution fits best (Figure 5d). With Cf, the rejection frequency of the AD test is very small (Figure 5e). The rejection frequency of the S-W test is best from SPI 1 to 12 for the Gamma distribution and for SPI 24 (3.79%) for the Logistic distribution (Figure 5f).

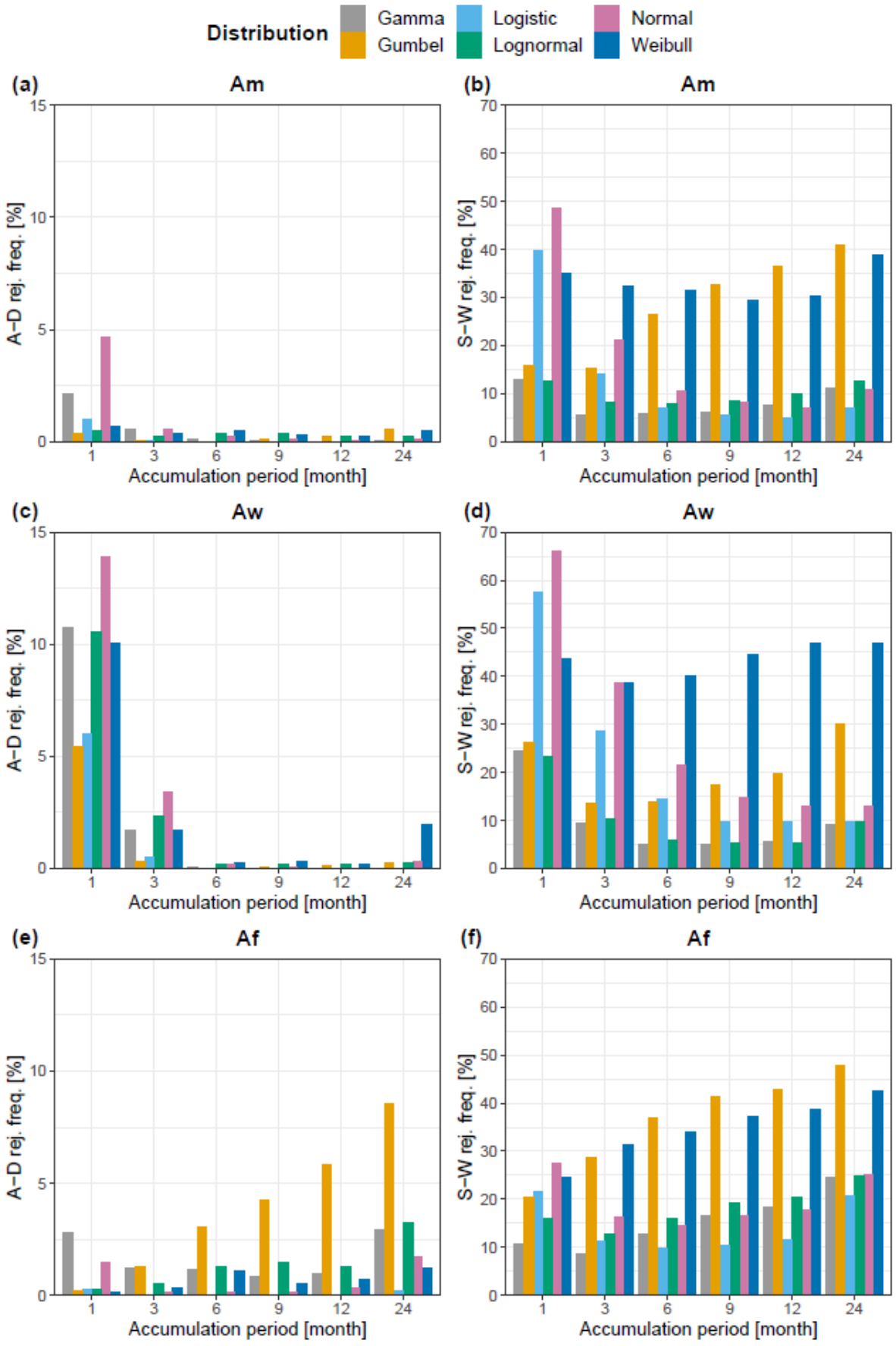

Figure 4: Rejection frequencies (%) for Anderson–Darling (A–D) and Shapiro–Wilk (S–W) test for all tested distributions and SPI accumulation periods over the tropical climate classes Am (monsoon), Aw (savannah) and Af (rainforest)

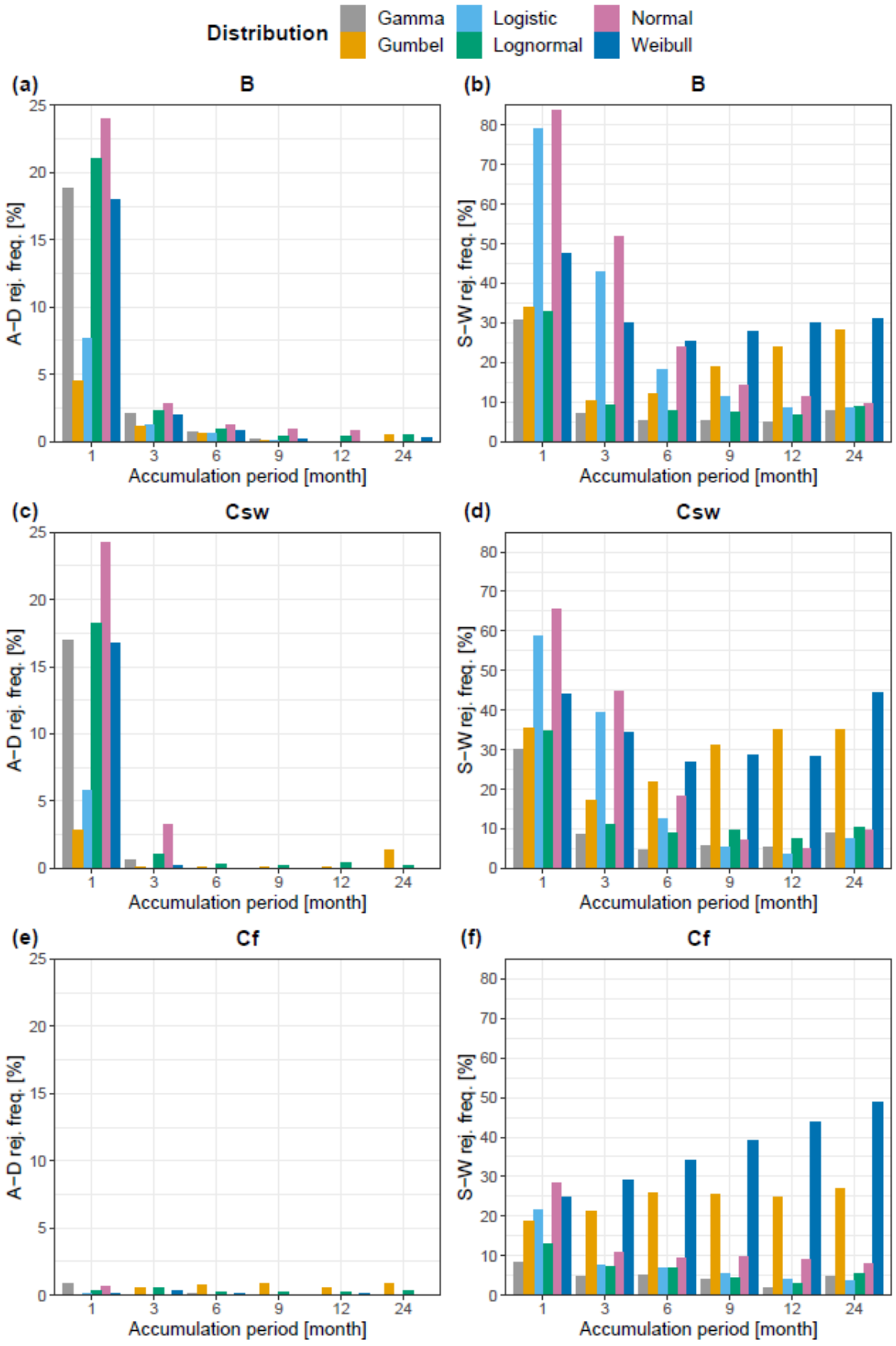

Figure 5: Rejection frequencies (%) for Anderson–Darling (A–D) and Shapiro–Wilk (S–W) test for all tested distributions and SPI accumulation periods over the tropical climate classes Am (monsoon), Aw (savannah) and Af (rainforest)

3.3 Rejection frequency of candidate distribution functions over the year

For a better understanding of the rejection frequencies of the best distributions according to the A-D and S-W test (Gamma Figure 6, Logistic Figure 7, Lognormal Figure 8), these were mapped together with the average precipitation over the course of the year. The Gamma distribution for Am SPI 1 has a slight increase of the rejection rate for the months of January to April with 21.8% to 26.7%, in which the mean precipitation is lowest. For the following months up to and including November, the rejection frequency of the 24-month accumulation period is highest, but not prominent (Figure 6a). For Aw, a high rejection rate can be seen in SPI 1 (28.4% to 50.4%) and SPI 3 (10.4% to 25.1%) from January to April. In November (22.4%) and December (43.2%) the rejection rate of SPI 1 is increased. In these months, the lowest mean precipitation falls (Figure 6b). The highest values of the rejection rates of the climate zone Af. occur in SPI 24 with rejection rates between 20 and 30% (Figure 6c). The distribution of the rejection frequency in B is similar to Aw. They are high for SPI 1 (33.4% to 67.0%) and 3 (5.4% to 17.0%) in the months January to April and for SPI 1 again in November (41.9%) and December (60.5%). The overall values are higher than for climate zone Aw. In addition, in this climate zone the average precipitation is lowest in the months with the high rejection rates (Figure 6d). Also climate zone Csw follows the pattern of Aw and B with the highest rejection rate of the Gamma distribution in January for SPI 1 (69.4%) (Figure 6e). Cf has consistently low rejection rates without abnormalities (Figure 6f).

For Am the rejection frequency of SPI 1 (29.8% to 65.9%) and SPI 3 (17.6% to 31.6%) is increased from January to May and for SPI 1 again from September to December (20.5% to 54.4%). The high rejection rates do not only occur during low mean precipitation but also in transitional periods where precipitation increases or decreases. The SPI 1 has the highest rejection rate in each month (Figure 7a). Aw has increased rejection rates for SPI 1 throughout the year (28.0% to 85.8%), from January to May (10.7% to 82.3%) also for SPI 3 and in April (36.1%)/May (24.8%) for SPI 6. In this case as well, SPI 1 has the highest rejection rate every month (Figure 7b). For climate zone Af, the rejection rate for SPI 1 is increased in January (39.4%) and February (45.5%). Otherwise the rejection rates are low for all accumulation periods throughout the rest of the year. Between April and July they are even lower than the rejection rates for Gamma and Lognormal distribution (Figure 7c). Climate zone B has increased rejection rates for SPI 1 throughout the whole year (51.8% to 98.9%) and for SPI 3 from January to June (30.5% to 96.8%) as well as in November (35.5%) and December (32.2). The values for SPI 6 are also relatively high in February (49.2%), May (34.8%) and June (25.6%) (Figure 7d). The distribution of rejection rates for Csw is almost like B, SPI 1 has high

values (between 21.6% and 99.2%) except June/July and so does SPI 3 (between 18.7% and 92.5%). The rejection rate of SPI 6 is higher in February (32.8%), April (32.8%) and May (41.1%) (Figure 7e). In contrast, Cf has almost consistently low rejection rates. They are only increased for the months of January (45.5%), February (31.8 %), June (41.8%) and July (34.5%) at SPI 1 (Figure 7f). With several values above a 90% rejection rate, the Logistic distribution has the highest overall rejection rates, especially the rejection rate in the climate zones B (maximum 98.9%) and Csw (maximum 99.2%). Generally, the rejection rates are higher when the mean annual precipitation is low, but high rejection rates also occur during transitions from wet to dry months and vice versa.

The Lognormal distribution shows no abnormalities for the climate zone Am. The rejection frequencies remain equally low throughout the year (Figure 8a). For climate zone Aw, however, the rejection frequency is increased from January to May (between 24.7% and 38.6%) and from October to December (between 20.5% and 30.4%). The rejection rates are lower than in the Gamma and Logistic distribution but increased over a longer period than in the Gamma distribution. The increased rejection rates overlap with low mean precipitation but also with transition periods to higher precipitation (Figure 8b). The rejection frequency for Af is constantly between 20% and 30% for most months with the worst represented accumulation period of 24 months. The average rainfall in these climates has few fluctuations and no dry period (Figure 8c). B has a high rejection rate for SPI 1 from January to May (between 18.1% and 69.7%) and in November (56.3%)/December (54.5%), like climate zone Aw. For SPI 3 the rejection rate for December is higher than in the other months. Again, the high rejection rates for small accumulation periods coincide with periods of low precipitation (Figure 8d). The situation is similar for climate zone Csw (SPI 1 January to June between 25.7 and 70.1%), whereby the accumulation periods 1, 3, 6 and 9 have relatively high rejection rates in June (between 21.2% and 27.0%) and July (between 9.5% and 23.2%). These months have a high precipitation with 150 to 200 mm (Figure 8e). The rejection frequency for Cf is relatively constant. Only for the months of March (21.8%), August (18.2%), October (25.5%) and December (28.2%) is the SPI 1 slightly increased. The rejection frequency for Cf is relatively constant. Only for the months of March (21.8%), August (18.2%), October (25.5%) and December (28.2%) the SPI 1 is slightly increased. The SPI 3 is marginally increased in July (17.3%) and August (13.6%) (Figure 8f). The results of the other distributions are displayed in Supporting Information Gumbel (Figure S 1), Normal (Figure S 2), and Weibull (Figure S 3) as well as the A-D test (Figure S 4 to Figure S 9).

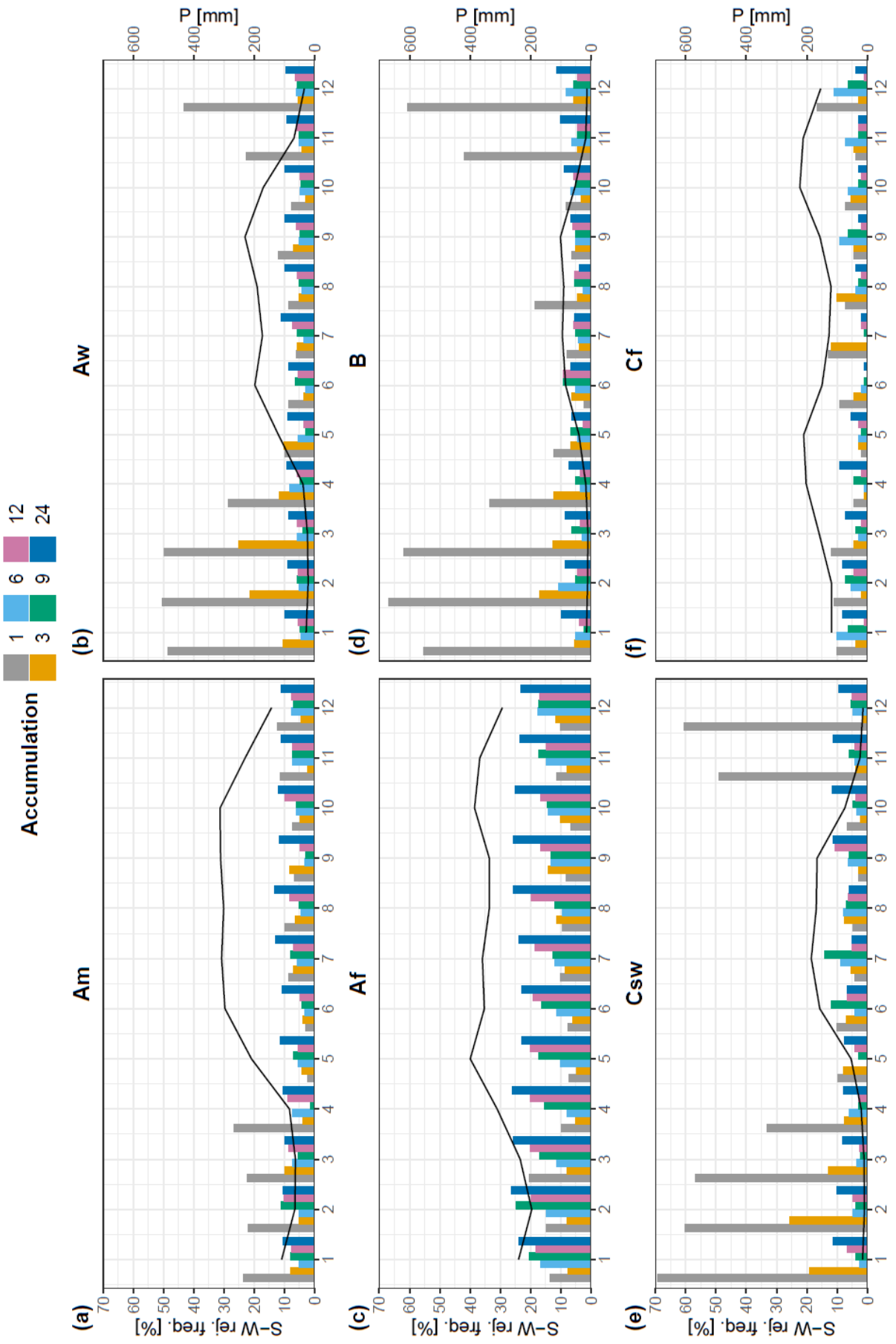

Figure 6: Rejection frequency of the S-W test of the Gamma distribution per accumulation period during the year and the mean annual precipitation for the climate zones Am, Aw, Af, B, Csw and Cf

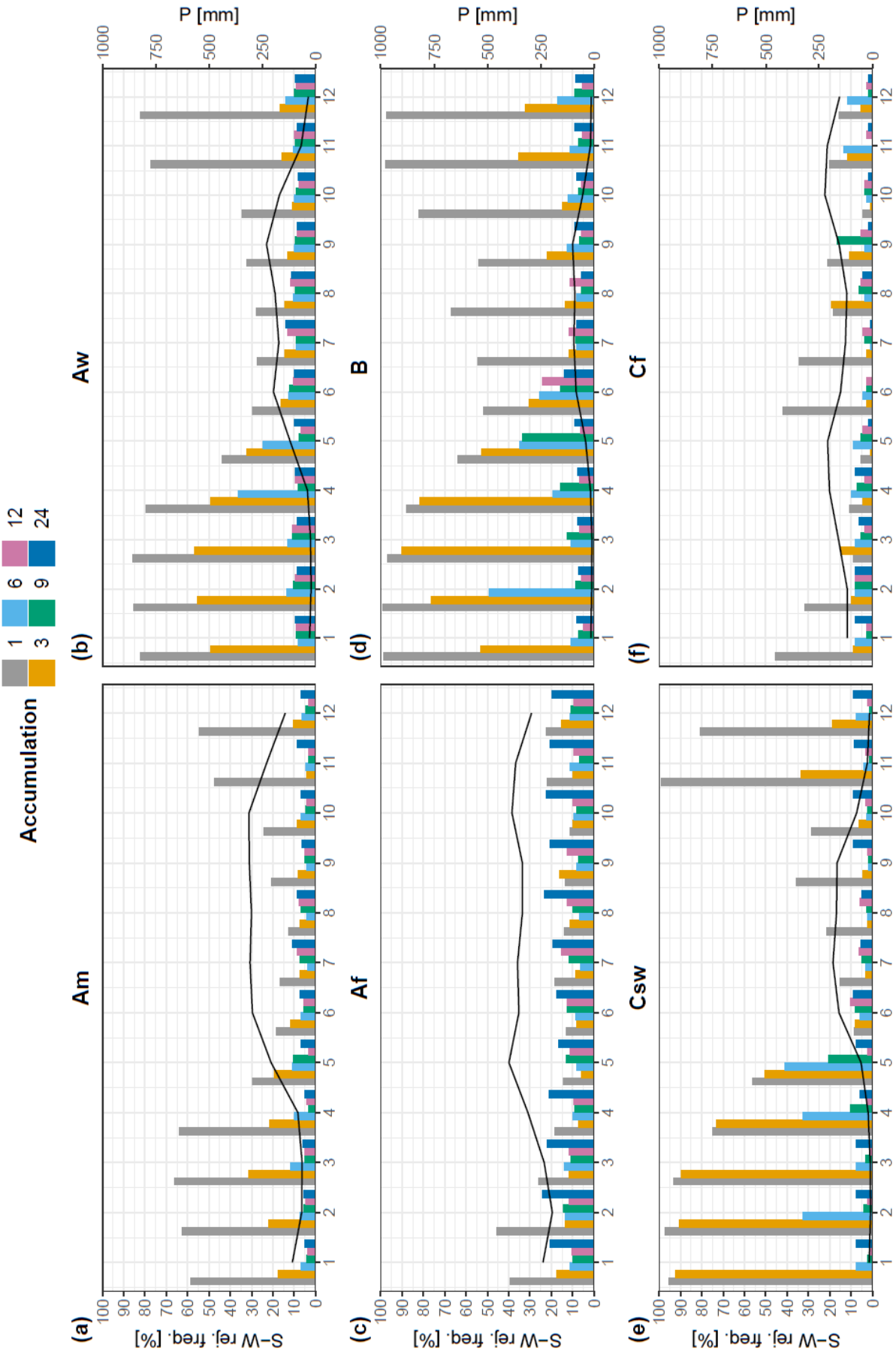

Figure 7: Rejection frequency of the S-W test of the Logistic distribution per accumulation period during the year and the mean annual precipitation for the climate zones Am, Aw, Af, B, Csw and Cf

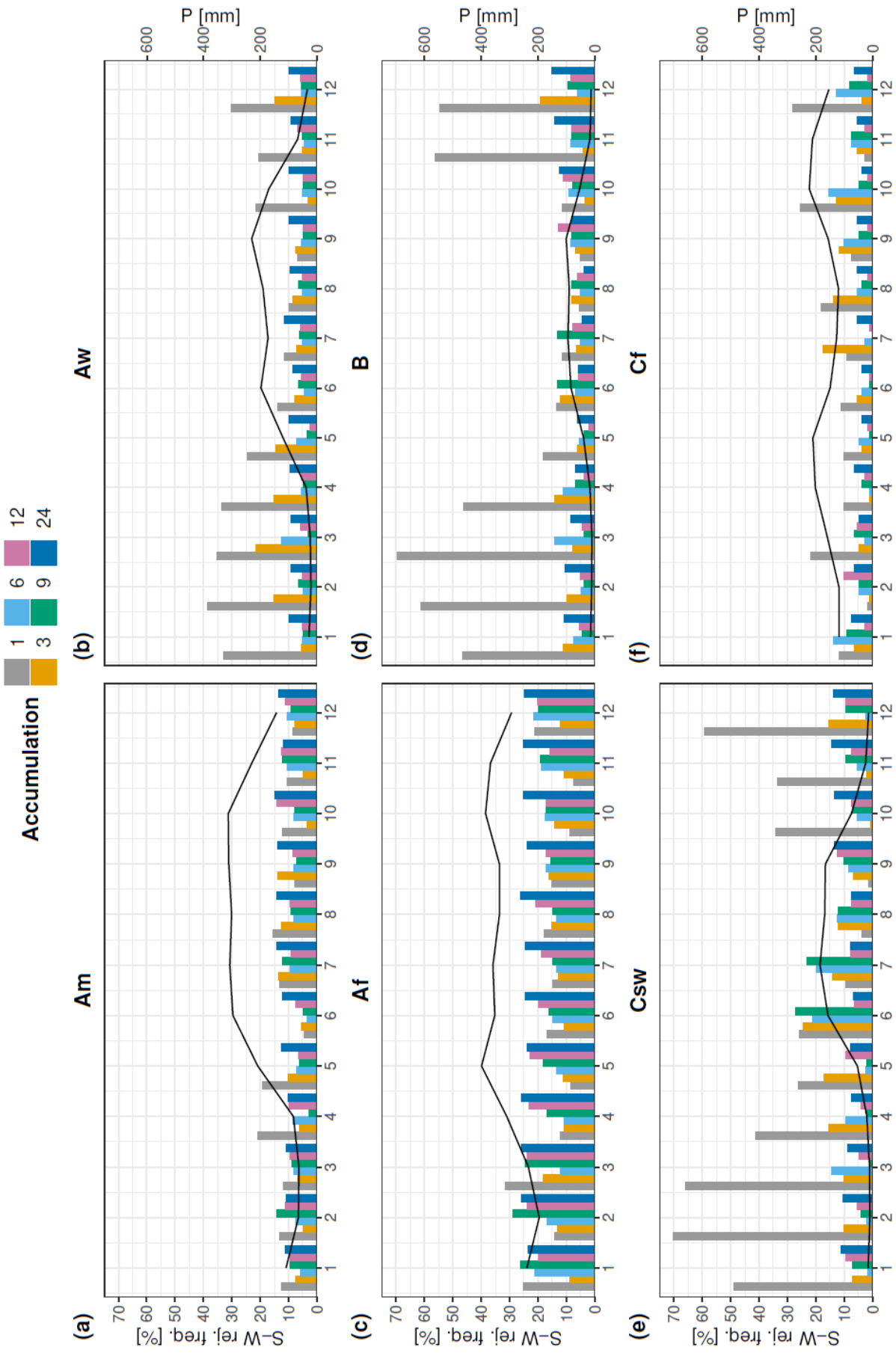

Figure 8: Rejection frequency of the S-W test of the Lognormal distribution per accumulation period during the year and the mean annual precipitation for the climate zones Am, Aw, Af, B, Csw and Cf

3.4. SPI distribution fitting with AIC

Due to the differences in rejection rates, especially for SPI 1, between dry (January, February, March) and wet periods (July, August, September), the best fitting distributions according to AIC were considered separately for these periods (Figure 9). For the dry period SPI 1, it is noticeable that on the west coast of Mexico and Honduras, as well as in Costa Rica and Panama, the Lognormal distribution predominates, which in total makes up the largest part with 42.7% of the land mass. For the climate zones Am and Aw, it is the most common distribution with a share of over 50% (Figure 10a and Figure 10c). On the east coast of Mexico and Nicaragua, the Gumbel distribution dominates. It is the third most common distribution with 17.2%. In the central area between the coasts and in Columbia, the Gamma distribution is the best fitting distribution. In total it has a share of 35.2% of the land mass and is therefore the second most common distribution. It has the highest compartment as the best fitting distribution for all climate zones except Am and Aw. In the wet season there is a similar pattern of distribution, but the Lognormal and Gumbel functions are less common. They occur mainly along the coasts of Mexico. A large part of the area is best represented by the Gamma distribution, 43.2% in total. The only climate zone where a different distribution fits better than the Gamma is Aw, where the Lognormal distribution fits best in 54.0% (Figure 10b). The Lognormal distribution also dominates the dry period SPI 3 with 39.7%, which is the best fitting distribution of the climate zones Aw (41.6%, Figure 10c), B (66.5%, Figure 11a) and Csw (75.5%, Figure 11c). The second-best fitting distribution is the Gamma distribution with 37.1%, which fits best for the climate zones Af (44.7%, Figure 10e), Am (48.4%, Figure 10a) and Cf (44.5%, Figure 11e). During the wet season SPI 3 (39.3%) and SPI 6 (32.2%) the Gamma distribution often is the most appropriate distribution for all climate zones. This is the case for SPI 6 in the dry season (39.0%) as well. Furthermore, for SPI 9 of this season the Gamma distribution fits most often with 26.0% of the land mass. However, for Af the Weibull distribution (20.0%, Figure 10e) and for Aw the Lognormal distribution (26.1%, Figure 10c) mostly fits. In SPI 9 of the wet season, the Gamma distribution is the most common distribution with 28.5% of the landmass. In contrast, the Af and Cf climate zones state the Gumbel distribution of 21.8% (Figure 10f) and 29.1% (Figure 11f) respectively as the best fitting distribution. SPI 12 and SPI 24 of the dry season have the Lognormal distribution as the most appropriate distribution with 25.7% and 23.7%. In climate zone B (Figure 11a), the Gamma distribution is only 25.8% (SPI 12) and 23.0% (SPI 24). In the wet season, the Gumbel distribution at SPI 12 (25.35%) and 24 (23.27%) is the most suitable. In both cases, this is also true for the Af and Aw climate zones and for SPI 12 for Cf. The best distribution for each climate zone differs from one another. The distribution

pattern is heterogeneous. Overall, the percentages of the best fitting distribution become smaller as the accumulation period increases.

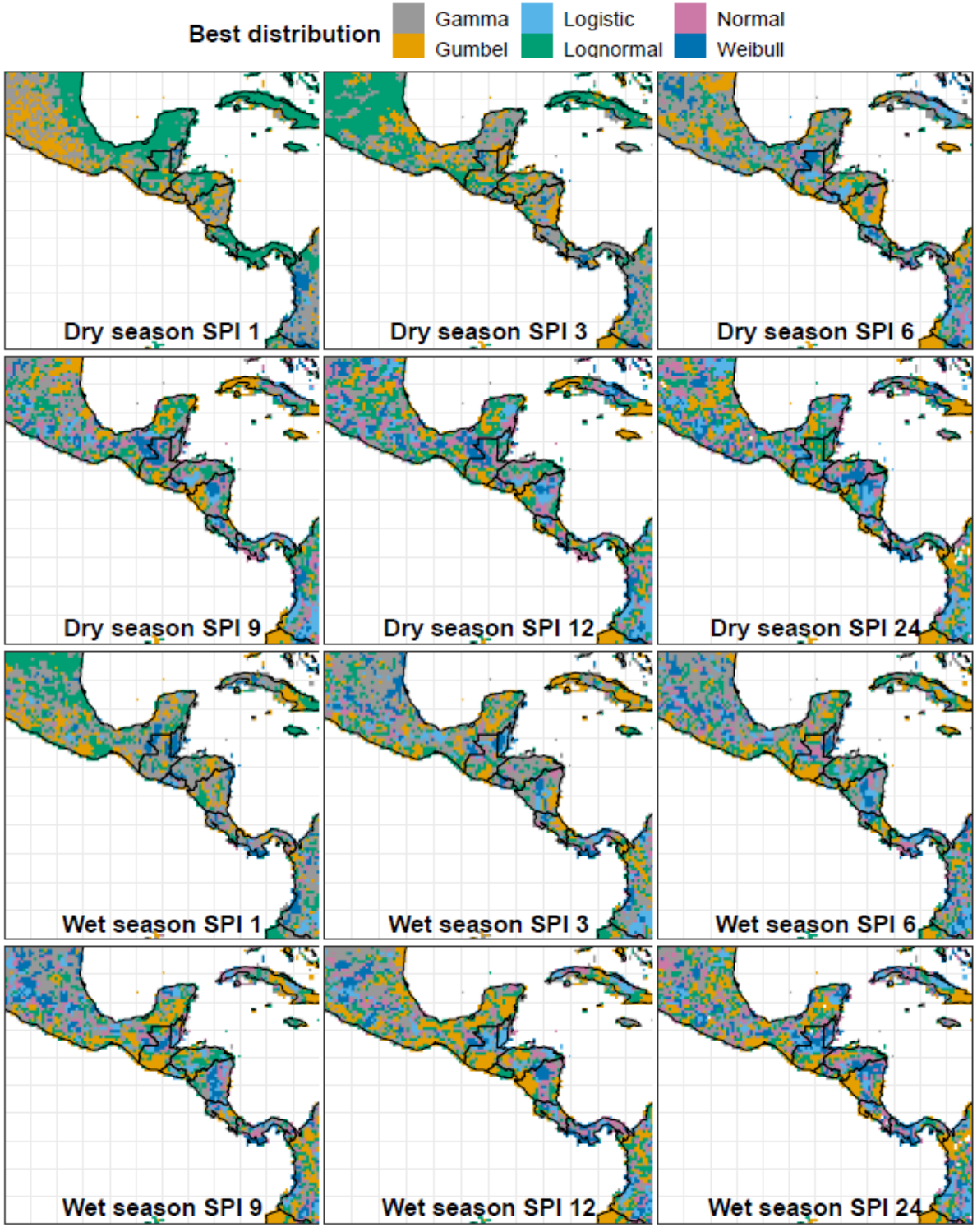

Figure 9: Best distribution of dry (January, February, March) and wet period (July, August, September) according to AIC for SPI 1, 3, 6, 9, 12 and 24

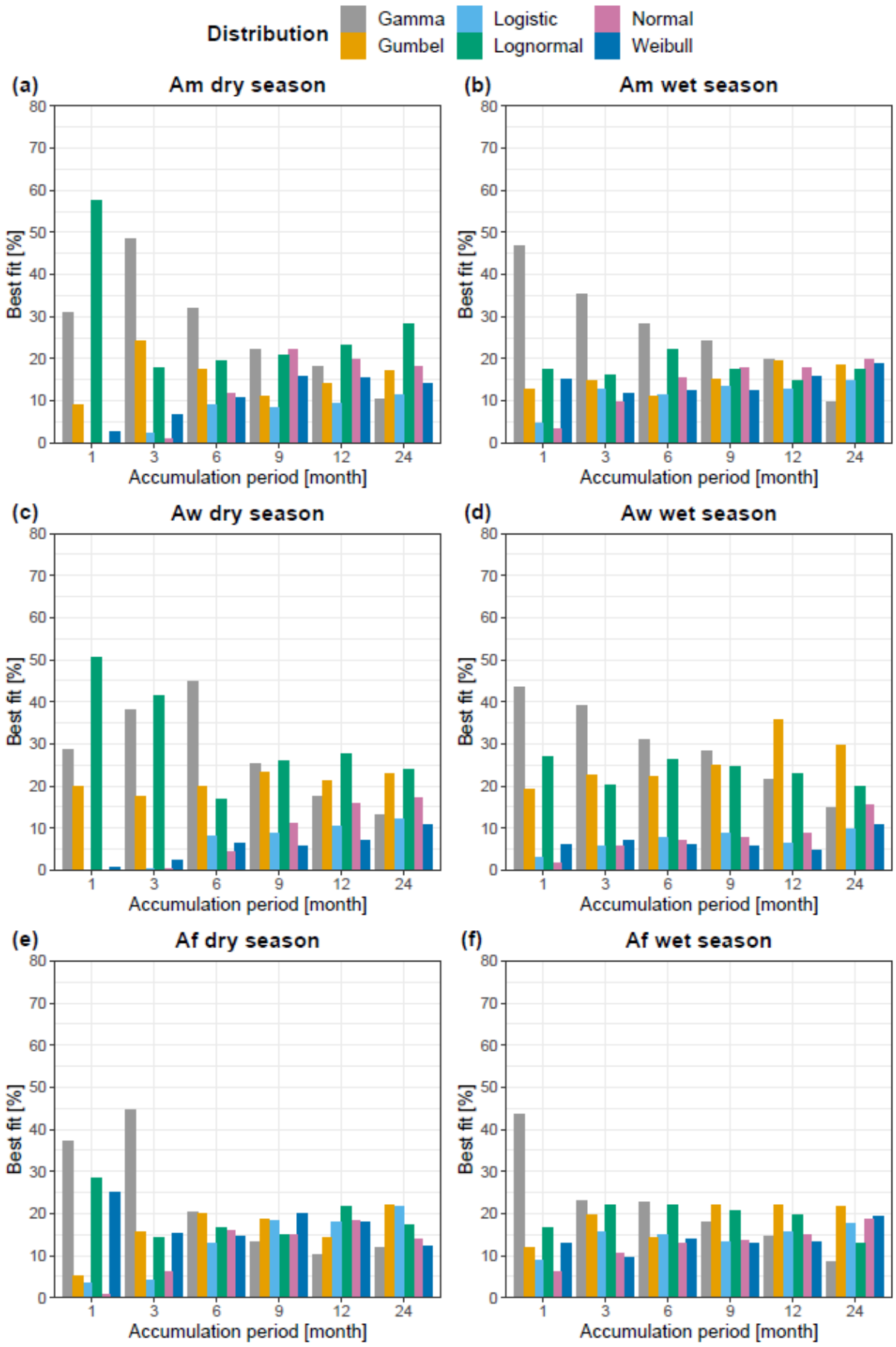

Figure 10: Best distribution according to AIC [%] per climate zone Am, Aw and Af of dry (January, February, March) and wet period (July, August, September) for accumulation period 1, 3, 6, 9, 12 and 24

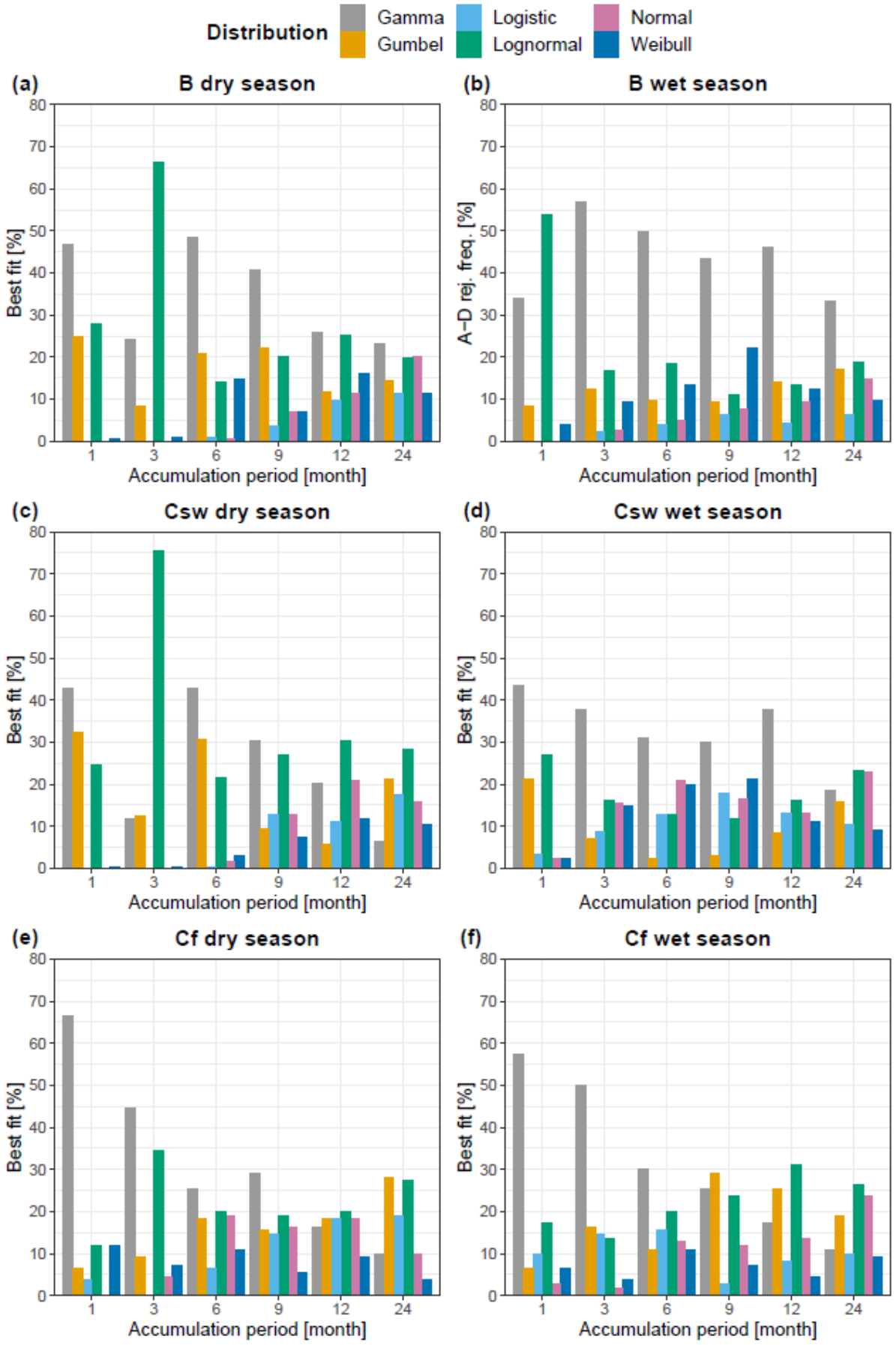

Figure 11: Best distribution according to AIC [%] per climate zone B, Csw and Cf of dry (January, February, March) and wet period (July, August, September) for accumulation period 1, 3, 6, 9, 12 and 24

3.5 SPI values for different distributions on July 2014

Figure 12 shows the SPI in July 2014 of accumulation periods 1, 6 and 12 for the Gamma, Logistic, Lognormal and the best fitting distribution, according to AIC. The spreading of drought corresponds to the distributions for the respective accumulation period. In SPI 1 almost the whole surface of Central America is affected, only parts of Northern Mexico and Costa Rica have positive SPI values. In contrast, the drought in SPI 6 is mainly concentrated in El Salvador, Honduras and Nicaragua. Southern parts of Mexico, Panama and Columbia are also affected by drought. Regarding SPI 12, a positive SPI predominates in Mexico, while drought is only found in Nicaragua, Panama and southern Honduras. A difference between the distributions is visible in the intensity of the drought. The Logistic distribution estimates the drought to be the least extreme, so the SPI values are higher than in the Gamma and Lognormal distribution. In terms of the Gamma and Lognormal distribution, it is noticeable that the Gamma distribution especially at SPI 1 classifies single points as extremes, while the Lognormal distribution represents a smoother transition. The SPI values of the best fit lies between Logistic and Gamma/Lognormal distribution. They estimate the drought to be stronger than the Logistic but weaker than the Gamma/Lognormal distribution.

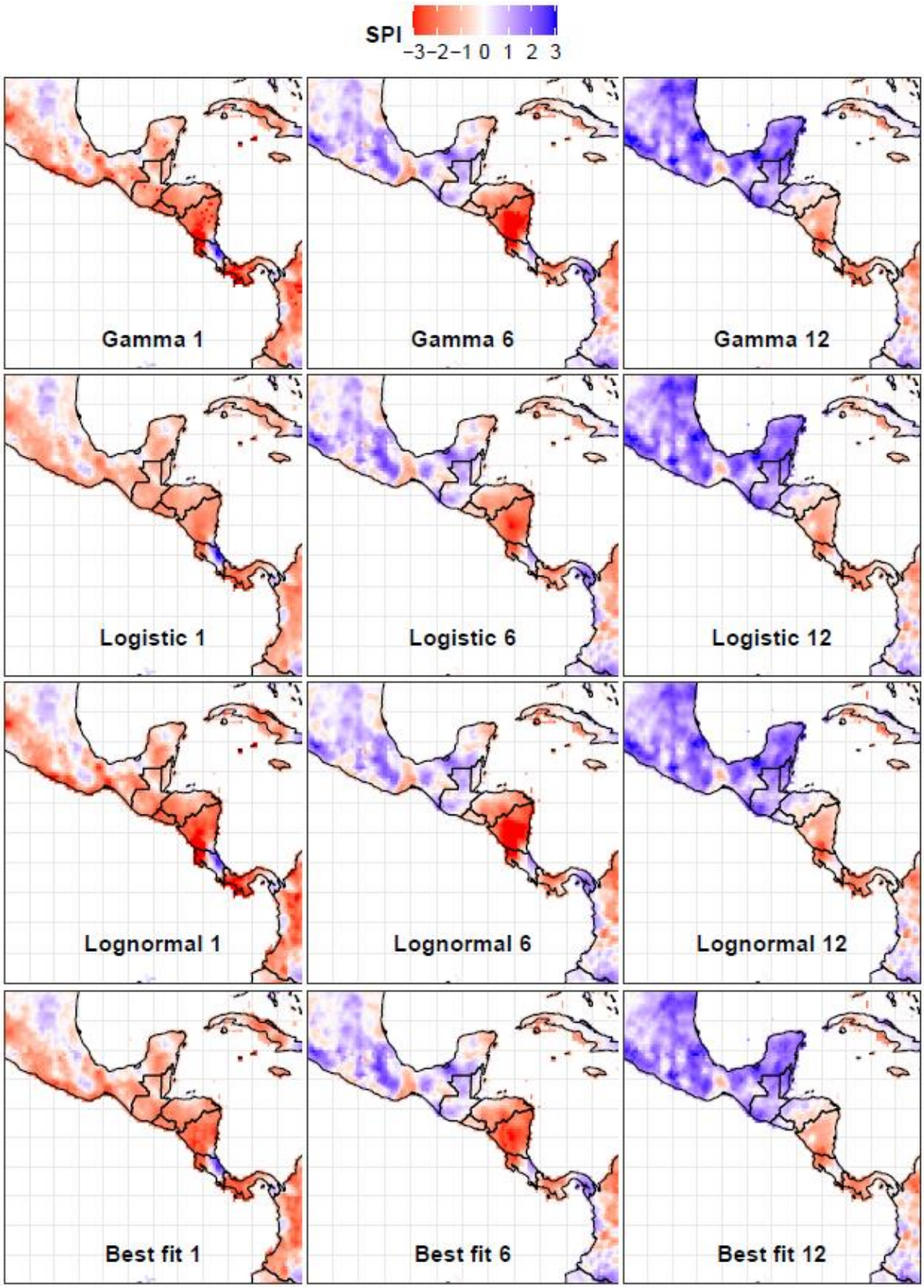

Figure 12: SPI in July 2014 of accumulation periods 1, 6 and 12 for the Gamma, Logistic, Lognormal and the best fitting distribution, according to AIC

3.6 Severe and extreme drought from 2014 to 2016

The drought from 2014 to 2016 is visualized as a drought area in % (threshold SPI < 1.5) with Gamma, Logistic, Lognormal and best fit distribution according to AIC (Figure 13). The analysis is carried out for SPI 1, SPI 6 and SPI 12. In terms of area, the drought in 2014 reaches two peaks in April and July. The largest area under drought follows in mid-2015, depending on the climate zone between May and August. The peak of climate zone Am is three months after Cf has reached the peak. From the main peak on, the area under drought slowly shrinks until it reaches a low point in November/December. In February 2016, another peak follows with steep ascent and descent. It mainly affects the Af and Cf climate zones. Overall, B and Csw are the least affected by the drought. The area below is the largest for Cf, Am and Af. With a maximum area under drought of 61.8% of Cf, the Gamma distribution estimates the drought as the largest, followed by Lognormal with 60.0%, best fit with 58.1% and finally Logistic with 47.2%. The area under drought at SPI 6 has a smaller peak in mid-2014, which extends from July to December 2014. The main peak is in September 2015 with a rapid increase and a slow decrease until the end of 2016. Also at SPI 6, climate zones B and Csw are the least affected by drought. The area under drought is larger for Cf and Af than for SPI 1, while B and Csw are less affected. The maximum peaks of Cf are very close together with 70.0% for Gamma, 69.0% for Logistic, 70.9% for Lognormal and 70.9% for best fit. However, the area under drought for Am, Af and Aw is significantly smaller in Logistic distribution than the others. In SPI 12, instead of two separate droughts, there is one which has its peak in February 2016. In contrast to the shorter accumulation periods, there is a slower increase since July 2014 and a stronger decrease at the end of 2016. Particularly affected by drought are the climate zones Cf, Am and Af. Meanwhile B and Csw have almost no drought as for SPI 6. The Logistic distribution estimates the area under drought again to be smaller than the other distributions. The main peak of Cf is almost the same as for SPI 6, around 70%, except for the Logistic distribution with 60%.

To better understand the differences between the individual distributions and the best fit according to AIC in an area under drought (AUD), Figure 14 and Figure 15 were created. were created. The deviation was calculated by AUD best fit minus AUD distribution, i.e. a positive deviation indicates that AUD is smaller than the best fit and a negative deviation shows that it is larger. They demonstrate the differences of the area under drought from Gamma in %, Logistic and Lognormal distribution to the best fit for each climate zone. Overall, the Logistic distribution has the highest deviation for all climate zones and all accumulation periods. The Gamma and Lognormal distribution have a similar deviation and fluctuate around 0 with up to 5% of deviation.

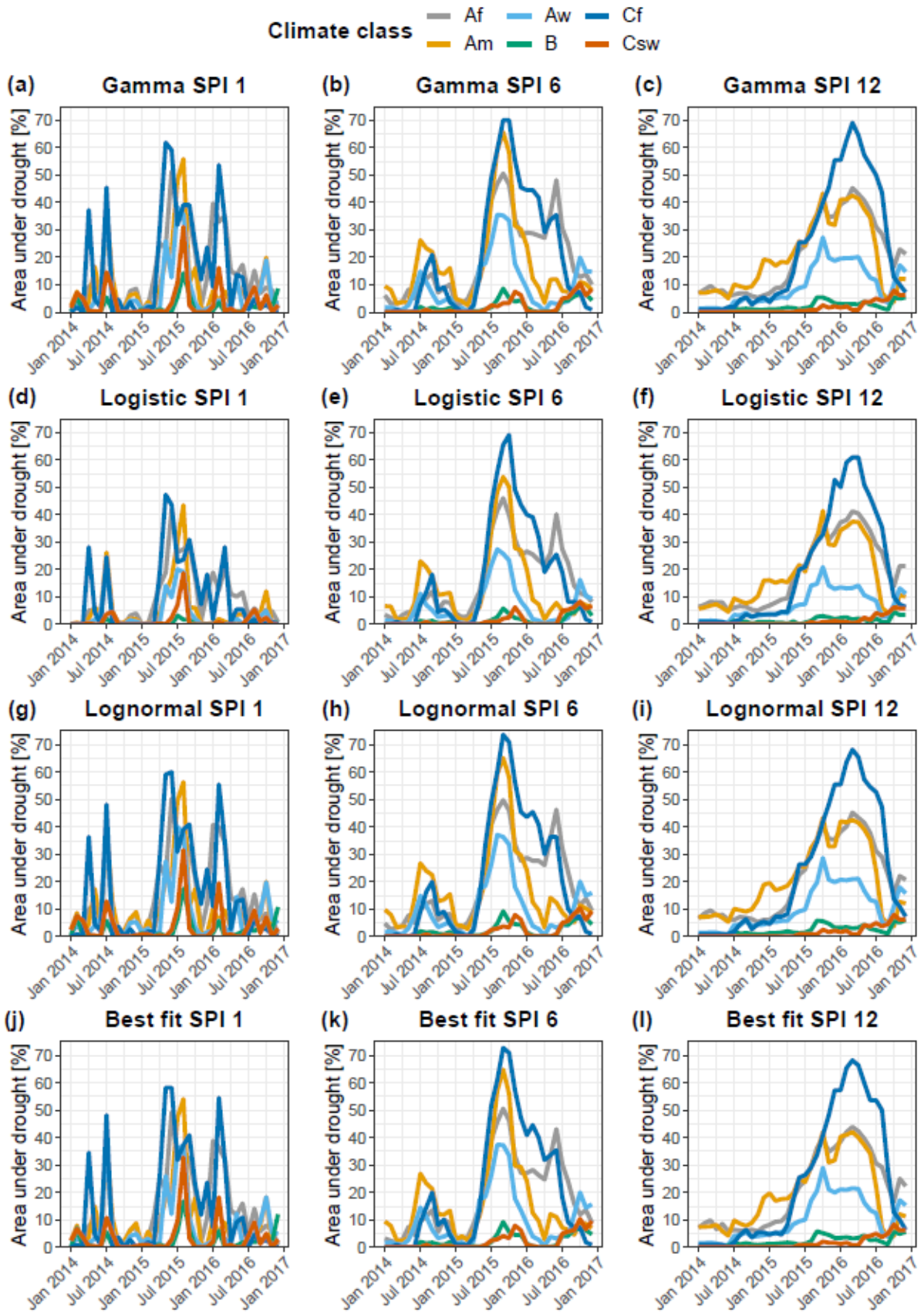

Figure 13: Area und drought [%] (threshold: SPI < 1.5) of SPI 1, SPI 6 and SPI 12 for Gamma, Logistic, Lognormal and best fit per Grid distribution, according to AIC

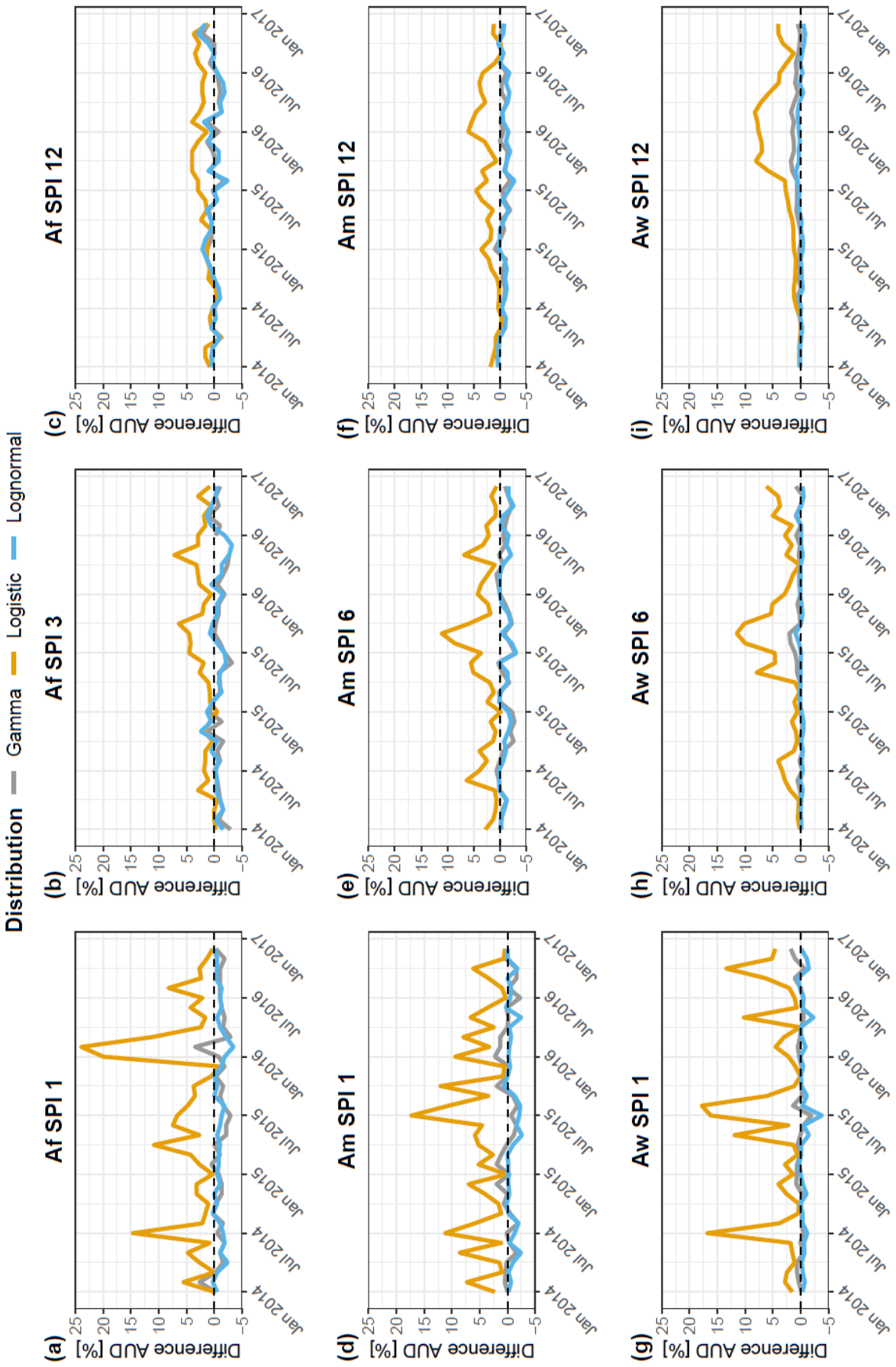

Figure 14: Difference AUD [%] between a certain distribution and the respective best fitting distribution with accumulation periods 1, 6 and 12 for the climate zones Af, Am and Aw

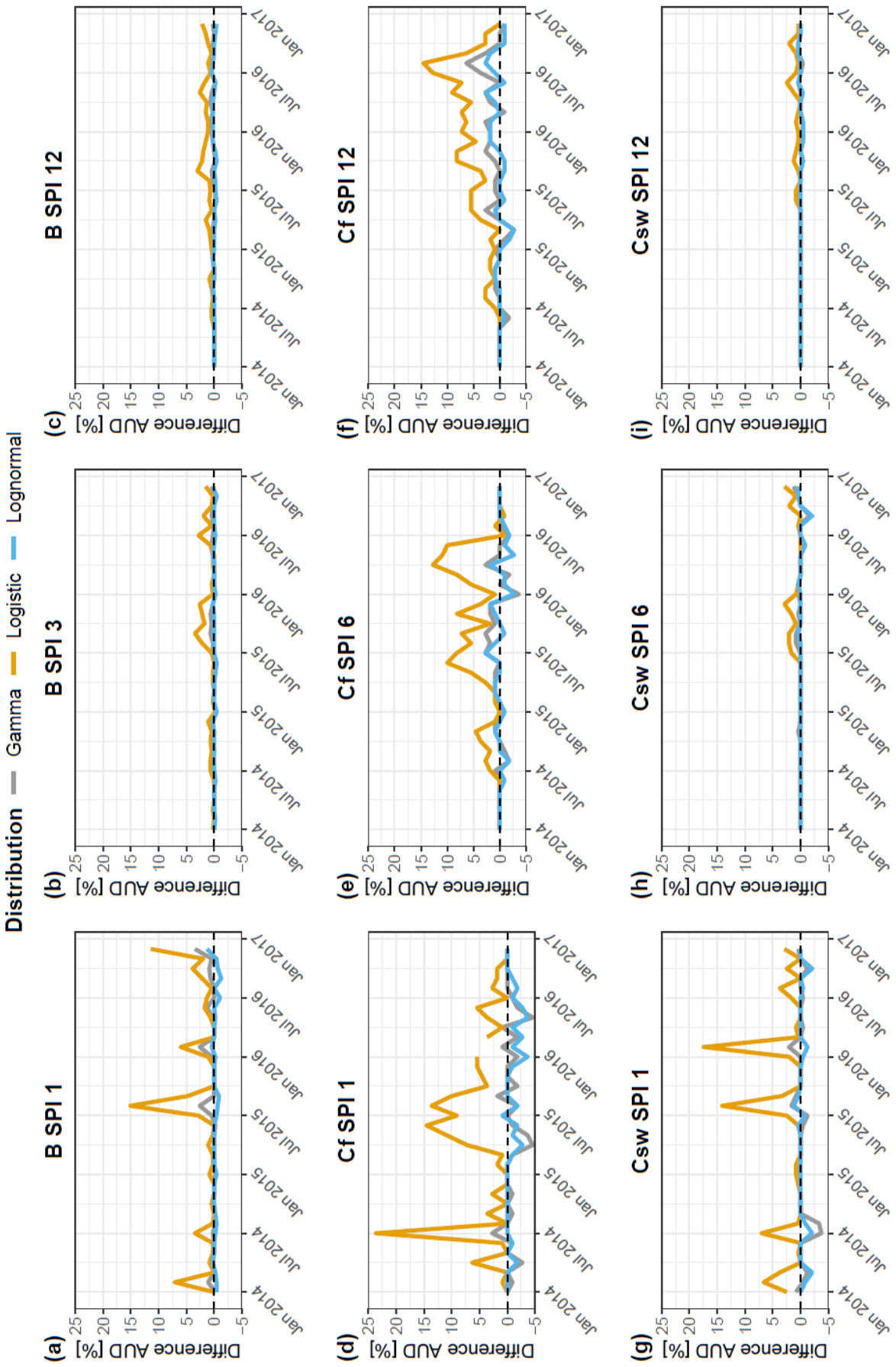

Figure 15: Difference AUD [%] between a certain distribution and the respective best fitting distribution with accumulation periods 1, 6 and 12 for the climate zones B, Cf and Csw

4. Discussion

This work found that in the assessment of drought conditions with the SPI, the standard-use Gamma distribution, which has been developed for the mid-latitude, is also appropriate for most of the tropical climate zones of Central America with some notable exceptions. The focus here is on the individual climate zones, which were calculated with the CHIRPS data which were also used for the SPI. Seasonal differences and differences between the accumulation periods of the climate zones are considered and discussed. Furthermore, differences in drought intensity between different distributions are analyzed.

4.1 Local variations of the climate zones in Central America

There have been many modifications proposed to the Köppen system (Essenwanger et al., 2001). The classification locks nearly like Beck et al. (2018), where the definition of climate zones was also taken from, and Kriticos et al. (2012). Af is the wettest tropical climate zone, followed by Am and Aw (Beck et al., 2018). On the east coast the average annual precipitation is higher than on the Pacific coast (Bundschuh et al., 2007). This corresponds to the results that most parts of Central America are tropical climates with Am on the west coast and Aw on the east coast. Af occurs in Costa Rica and Columbia. Globally seen, the tropical A climate class by land area is the third largest at 19.0%, and Aw represents the second most common individual climate class by land area at 11.5% (Peel et al., 2007). Guatemala has a moderate Cwb climate at an altitude of 1500 m. All surrounding areas are located in tropical climates, as Peel et al (2007). Other Parts of Columbia have got temperate climate zones in the mountain areas. In Mexico, there is an arid climate in the very southern part of the country. Moving to the North, the climate becomes more and more temperate. The complex horizontal topography means that a coarse horizontal resolution may have difficulties in describing the surface properties of Central America (Imbach et al., 2018). Beck et al (2018) use a 0.0083° resolution (approximately 1 km at the equator), which is smaller than the one used here with 0.25°x0.25°. In order to obtain suitable information, it would be useful to use the CHIRPS data in the lowest possible resolution (0.05°x0.05°).

4.2 Best fit of candidate distributions for Central America with A-D and S-W test

In general, the rejection rate for the A-D test in this study is very low compared to other studies (e.g. Blain et al. 2018; Stagge et al., 2015) and often below the significance level. A possible reason is that, in difference to this work, bootstrapping by Stagge et al. (2015) was used Due to this procedure, true uncertainty bounds could be produced. Furthermore, Stagge et al. (2015) used daily precipitation data, where the resulting accumulated values follow a similar right skewed Gamma distribution with a less extreme tail. This may result in different results with higher rejection frequencies, because the distribution of the extreme values is shifted by bootstrapping. The significance level of the A-W test therefore can be classified as low. The best distribution for SPI 1 over whole Central America is the Gumbel distribution for the A-D test, for the other accumulation periods the Logistic distribution is recommended. Stagge et al. (2015) have found that for short accumulation periods, the Weibull and Gumbel fits best. In the case of Stagge et al. (2015), the Weibull function was dominant, whereas in this work the Gumbel distribution is clearly more appropriate, according to A-D test. On the other hand, the S-W test recommends the Gamma distribution, except for SPI 24 where the Logistic function fits best. The results of the A-D test differ from previous studies, while the results of the S-W test confirm that the Gamma distribution describes wet and dry climate regions well (Blain et al., 2018; Guenang et al., 2019; Lloyd-Hughes and Saunders, 2002; McKee et al., 1993; Naresh Kumar et al., 2009; Stage et al., 2015; Sienz et al., 2012; Touma et al., 2015). However, the A-D test is inferior to the S-W test (Blain et al., 2018), which is why the S-W test can be considered more meaningful. In fact, the Gamma distribution has a relatively flexible shape parameter suitable for describing a range of accumulated precipitation distributions (Stagge et al., 2015; Wang et al. 2019). This also explains why the Gamma distribution for certain cases in this study best describes the values. The results of the S-W test for SPI 1 and SPI 24 are different from the studies mentioned above. In contrast to other studies, the Gamma distribution is also recommended for SPI 1 rather than the Weibull distribution. SPI 24 was not examined by the studies pointed out above. The climate in Europe is different from the tropics, in Central America the climate is mostly humid and tropical while Europe has a temperate climate (Beck et al., 2018) and could therefore produce different results. The Weibull and Gumbel distribution has the ability to model strongly distorted precipitation distributions, where most values are close to zero (Stagge et al., 2015). Due to the high humidity in the tropical climates of Central America, precipitation is rarely close to zero, which means that the Gamma and Weibull function lose their advantage over the Gamma distribution.

Regarding the climate zones individually, it is noticeable that for shorter accumulation periods (1 to 3 months) the Gumbel distribution is often recommended by the A-D test. This is true for the climate zones Am, Aw, B and Csw and is consistent for SPI 1 with the observation of Blain et al. (2018) and Stagge et al. (2015), who found the lowest rejection frequency for the Weibull and Gumbel function. The reason for this is the ability of the Weibull and Gumbel distributions to model strongly distorted precipitation distributions, where most values are close to zero (Stagge et al., 2015). The higher scored S-W test, however, especially emphasizes the Gamma distribution for shorter accumulation periods, as most previous studies did (Blain et al., 2018; Guenang et al., 2019; Lloyd-Hughes and Saunders, 2002; McKee et al., 1993; Naresh Kumar et al., 2009; Stage et al., 2015; Sienz et al., 2012; Touma et al., 2015). It is noticeable that for the climate zones Am, Af, Csw and Cf, the Logistic function has the lowest rejection rate at higher accumulation periods. This is not found in any other study so far. However, most of the other studies only consider accumulation periods between 1 and 12 months (Blaine et al., 2018; Stagge et al. 2015), instead of 1 to 24 months as considered in this case. Another notable feature is that the Lognormal distribution at SPI 1 of climate zone Aw has the lowest rejection rate for the S-W test; Wang et al. (2018) also found a best fit with the Lognormal distribution.

4.3 Variations of distribution fitting over the year

A high acceptance rate can be observed at the 6-, 9-, 12-, 24-month scales. For the 1 and 3-month scale, a relatively high acceptance was observed from May to October for all climate zones except B. Each of the three distributions show high rejection rates for the accumulation periods 1 and 3 in the dry period of the seasonal climate zones Am, Aw, Csw and the arid B. This is consistent with the results of Wang et al. (2019), who found low acceptance rates of the K-S test for accumulation period 1 for several months. Accumulation periods 3, 6, 9, 12 and 24, however, had very high acceptance rates (Wang et al., 2019). The rejection rates for the Logistic distribution are lower than in the Gamma but increased over a longer period for climate zones Aw, B and Csw. In contrast to the Gamma distribution, the rejection frequency for the Logistic distribution is therefore also increased in the transition months between the rainy and the dry season. The Logistic distribution shows the highest rejection frequencies. Periods with zero precipitation make it difficult to adjust the probability distribution for the SPI (Wu et al., 2007). The non-normally distributed SPI is caused by a high probability of cases with null precipitation represented in the mixed distribution and used in the SPI construction. Furthermore, the limited sample size in dry areas and during dry periods reduces the reliability of the SPI values (Wu et al., 2007). Therefore, in arid locations or during dry seasons, when the cumulative probability of zero precipitation is high, the SPI cannot indicate the occurrence of drought (Wu et al., 2007) or indicate the end of a drought period when no precipitation is present (Blain, 2012). This is consistent with the higher rejection rate in periods with less precipitation in this thesis.

Stagge et al. (2015) did not find a seasonal pattern among the rejection rates for different accumulation periods, which allows modeling the precipitation deficit of the whole year with a single distribution. However, Pieper et al. (2020) found larger seasonal differences in the performance of the investigated candidate PDFs, similar to the results in this thesis. In June and July, several accumulation periods for Gamma distribution and especially Lognormal distribution have an increased rejection rate. This may be due to the fact that the seasonal climate zones Cs (dry summer) and Cw (dry winter) (Beck et al., 2018) were combined in this study. The rainy period of Cs is coincident with the dry period of Cw and vice versa, which makes the precipitation data more scattered than when looking at the climate zones individually.

4.4 Best fit for Central America with AIC for wet and dry season

Based on the previous results, the best fitting distribution, calculated with AIC, was determined for the dry and wet season. To determine the best performing PDF, the use of relative ratings such as the AIC instead of A-D and S-W test is recommended (Stagge et al., 2015; Sienz et al., 2012). For the wet season, the results are consistent with the S-W test. Overall, the Gamma distribution fits best for accumulation periods 1, 3, 6 and 9. For every climate zone, the Gamma distribution is the best fit for accumulation periods 3 and 6 at least. Many other papers recommend the two parameter Gamma distribution for different regions of the world, mostly for accumulation periods between 3 and 12 month (Blain et al., 2018; Guenang et al., 2019; Lloyd-Hughes and Saunders, 2002; McKee et al., 1993; Naresh Kumar et al., 2009; Stage et al., 2015; Sienz et al., 2012; Touma et al., 2015). The best fit of the climate zones varies between Normal (Am), Gumbel (Aw & Af), Gamma (B) and Lognormal (Csw & Cf) for accumulation period 24 months. Also, the area to which the best fitting distribution applies decreases in percentage with increasing accumulation period. This is in line with the recommendation of Guenang et al (2019) to choose the best fit distribution function at each grid point from an accumulation period of 12 months on in order to expect good SPI results and thus a better description of the drought.

The result of this work differs from these papers, because it classifies the Gamma distribution as best fit even for short accumulation periods (1 month). The Gumbel distribution is expected as the best fit for accumulation period 12 and 24 for climate zone Aw, Af and the overall result. This is not consistent with previous studies, which showed the Gumbel or Weibull distribution to be suitable for short accumulation periods (Stagge et al., 2015). Typically, during accumulation periods of 1 or 2 months, strongly sloped distributions with a sharp, asymptotic density near the zero limit occur, which are not best represented by the Gamma distribution (Stagge et al., 2015).

For the dry period, the AIC indicates that the Lognormal distribution is best suited for short accumulation periods (1 and 3 months) and for long accumulation periods (12 and 24 months). In Europe, the log-normal distribution does not fit as well as the Gamma distribution (Llyoyd-Hughes & Saunders, 2002, Stagge et. al., 2015), this shows the relevance of this study. Because in different regions of the world, different distributions fit best (Blain et al., 2018; Stage et al., 2015; Sienz et al., 2012; Touma et al., 2015), it was important for Central America to make a new study. For medium accumulation periods (6 and 9 months), the Gamma distribution fits best, but the Lognormal distribution occupies second or third place, confirming the result of the

S-W test, which states that the rejection rates for the Lognormal distribution are lower than for Gamma, especially for the dry months of seasonal climates. This can also be noticed looking at the individual climate zones: for the seasonal climate zones Am, Aw and Csw the Lognormal distribution fits best for most accumulation periods. Angelidis et al. (2012) provide similar results, the study concludes that in Portugal for a 12 or 24 months accumulation period the Lognormal or Normal PDF can be used instead of Gamma. Gamma as well as Lognormal and Normal function lead to almost the same results. For the non-seasonal climate zones Af, B and Cf, the Gamma distribution fits best for most accumulation periods, especially for the shorter ones. The comparison of several seasons is more difficult if differences occur solely due to the adequacy of the transforming distribution (Sienz et al. 2012).

4.5 Differences in the severe of the drought 2014 to 2016

The reported distributions Gamma, Logistic, Lognormal and the most appropriate distribution for each grid according to AIC (best fit) show differences in the intensity of drought 2014 to 2016 for the investigated accumulation periods 1, 6 and 12. Gamma and Logistic estimate the drought to sometimes be weaker and mostly be stronger than the best fit. The choice of PDF can lead to overestimated or reduced SPI values and thus to potentially incorrect estimates of the timing, intensity and duration of droughts (Guenang et al., 2019; Stagge et al., 2015). SPI values calculated with the two-parameter Gamma distribution can underestimate the intensity of dryness and wetness when precipitation is very low or very high in other regions of the world (Kumar et al., 2009; Sienz et al., 2012). The deviation from best fit is greater for the Logistic distribution than for Gamma and Lognormal over all climate zones and accumulation periods. It underestimates the severity of the drought in relation to the best fit. Gamma and Lognormal distribution have very similar deviations from best fit. Also, in Angelidis et al. (2012) Gamma and Lognormal function give almost the same results.

For the short accumulation periods (1 and 6 months) the area under drought fluctuates more for all climate zones. For small accumulation periods (3 or 6 months), the SPI often moves above and below zero. If the period is extended to 12 or 24, the SPI reacts more slowly to changes in precipitation. Periods where the SPI is negative and positive become numerically fewer but longer in terms of time (McKee et al., 1993), which is consistent with the result of this work. On small time scales, each new month has a large influence on the period sum of the precipitation. The larger the accumulation period, the smaller the influence of each new month on the total sum can be estimated (McKee et al., 1993).

Chen et al. (2007) observed the largest area of severe drought especially for the 2014 primera season (April–August) for data during 2001–2014. This study also observed two peaks in the AUD between April and August 2014, but AUD in in mid-2015, depending on the climate zone between May and August. Drought Category severe drought with SPI Values -1.50 to – 1.99 only occur in 4.4% of time and extreme drought SPI Value ≤ -2 in 2.3 % of time (McKee et al., 1993). In the years 2015 to 2016, however, more than 50% of the time there were severe and extreme droughts on up to 60% of the area per climate zone. This means that the intensity of the drought exceeds expectations and shows how extraordinarily strong this drought period was.

5. Conclusion

The Standardized Precipitation Index (SPI) is a well-established and important index already used to quantify and compare meteorological drought events around the world. It evaluates and characterizes the precipitation ratio of a certain time period in relation to the respective normal values (Stagge et al.,2015). While distribution recommendations have already been made for various regions, Central America has not been considered yet in the existing literature. It is important to check the accuracy of fit when working in a firstly inspected region or with a new data set, because improper probability distributions have the potential to distort drought index values. This study evaluated the choice of an adequate univariate probability distribution to use in the normalization of SPI values in Central America based on three research theses. The first assumption evaluated with this thesis was:

I. *To derive the SPI, the Gamma (accumulation period ≥ 3) and Weibull distribution (accumulation period < 3) functions show the best performance for each of the tropical climate zones in Central America.*

This thesis cannot be confirmed, since the overall Gamma distribution fits best for both short and long accumulation periods. There are slight differences between the results of the A-D, S-W test and AIC. The AIC is the highest scored due to the use of relative ratings and is used for the recommendations as recommended by Stagge et al. (2015) and Sienz et al. (2012). There are differences in the seasons, which also disproves the second thesis:

II. *There are no seasonal differences in the adjustment of candidate distributions for the SPI for different accumulation periods in the climate zones of Central American.*

For the wet season (January to March) the Gamma distribution has a broad effectiveness in Central America and is best suited for accumulation periods of 1 to 12 months, with a consistently good fit across the entire width of the climate zones. This is consistent with the conclusions of previous studies. In the wet season, from accumulation period 1 month to 12 months, the Gamma distribution is recommended for calculating the SPI. For very long accumulation periods in general, the Gumbel distribution is better, but the result varies between the climate zones. In some events, the Gumbel (Aw & Af), Lognormal (Csw & Cf), Gamma (B) or Normal (Am) fits best. The area, to which the best fitting distribution applies, decreases in percentage with increasing accumulation period. This suggests that for very long accumulation periods, the best fit of the respective climate zone should be used to calculate the

SPI and not one distribution for all. Only for long accumulation periods, these distributions dominate during the wet period. For shorter accumulation periods they are irrelevant.

The evenly humid Af and Cf climates do not have seasonal differences, which can be concluded from the fact that the rejection rates are consistently good. Therefore, in the dry season (July to September) the dominant distribution is dependent on climate zones. In the non-seasonal climate zones Af, B and Cf, the Gamma distribution again fits best, especially for the accumulation periods 1 to 6 month. For longer accumulation periods, the best distribution varies between Gumbel, Gamma and Lognormal distribution, as it does in the wet period. For the seasonal climate zones Am, Aw and Csw the Lognormal distribution dominates for short and long accumulation periods. For medium accumulation periods (3 and 6) the Gamma distribution is best suited, but the Lognormal distribution follows on the wide space. With regard to the last thesis, it is possible to recommend the Lognormal distribution for all accumulation periods in the dry period of the seasonal climate zones. Finally, the thesis puts forth, that:

III. Various distributions estimate the area under drought (SPI < 1.5) differently compared to the best fit (for each grid cell, the best fit distribution according to AIC is used to calculate the SPI).

The Logistic distribution has the largest deviation to the best fit compared to the Gamma and Lognormal distribution. The difference to the AUD of best fit is similar for Gamma and Lognormal distribution, considering the seasonal climates Am, Aw and Csw the Lognormal distribution fits marginally better than the Gamma distribution. This reinforces, that the Lognormal distribution is recommended for all accumulation periods in the dry period of the seasonal climate zones. Based on the intensity of the drought of 2014 to 2016 over time, it can be considered exceptionally strong.

The last step is an analysis of open questions. This study deals with the implementation of drought monitoring with one considered drought period, but drought characterization is also important. It would be interesting to analyze droughts over the whole time series to better estimate their intensity, for example, a drought ranking could be created and trends analyzed. With regard to current studies, a comparison with three parameter PDFs, especially exponentiated Weibull distribution would be an interesting continuation of this study. Pieper et al. (2020) evaluate SPI time-series over the global land area and for each continent individually during winter and summer, comparing two parametric PDFs with three-parametric ones. They recommended the use of the exponentiated Weibull distribution, which maximizes the

normality of SPI time-series in observations and simulations. Another aspect to consider is the comparison and distribution fitting with the Standardization Precipitation Evaporation Index (SPI). Many previous studies considered the SPI and SPEI in one work (e.g. Blain et al., 2018; Stagge et al., 2015; Wang et al., 2019), the advantage of the SPEI is the inclusion of the evaporation, which is not important in the SPI.

All in all, there is a difference between the accumulation periods 1 to 12 months and the very long accumulation period 24 months as well as a difference between the dry and rainy season of the seasonal climate zones Aw, Am and Csw. The Gamma distribution is recommended all year round for the non-seasonal climate zones Af, B and Csw and in the wet season of the seasonal climate zones Aw, Am and Csw of accumulation period 1 month to 12 months. For the very long accumulation periods (24 months) the SPI should be calculated with the most appropriate distribution for each grid cell. The Lognormal distribution is recommended for all accumulation periods in the dry period of seasonal climates.

VII References

Acosta, P., Almeida, R., Gindling, T., Lao Pena, C., 2017. Toward More Efficient and Effective Public Social Spending in Central America. The World Bank. https://doi.org/10.1596/978-1-4648-1060-2

Aguilar, E., Peterson, T.C., Obando, P.R., Frutos, R., Retana, J.A., Solera, M., Soley, J., García, I.G., Araujo, R.M., Santos, A.R., Valle, V.E., Brunet, M., Aguilar, L., Álvarez, L., Bautista, M., Castañón, C., Herrera, L., Ruano, E., Sinay, J.J., Sánchez, E., Oviedo, G.I.H., Obed, F., Salgado, J.E., Vázquez, J.L., Baca, M., Gutiérrez, M., Centella, C., Espinosa, J., Martínez, D., Olmedo, B., Espinoza, C.E.O., Núñez, R., Haylock, M., Benavides, H., Mayorga, R., 2005. Changes in precipitation and temperature extremes in Central America and northern South America, 1961–2003. J. Geophys. Res. 110, D23107. https://doi.org/10.1029/2005JD006119

Akaike, H., 1974. A New Look at the Statistical Model Identification, in: Parzen, E., Tanabe, K., Kitagawa, G. (Eds.), Selected Papers of Hirotugu Akaike, Springer Series in Statistics. Springer New York, New York, NY, pp. 215–222. https://doi.org/10.1007/978-1-4612-1694-0_16

Angelidis, P., Maris, F., Kotsovinos, N., Hrissanthou, V., 2012. Computation of Drought Index SPI with Alternative Distribution Functions. Water Resour Manage 26, 2453–2473. https://doi.org/10.1007/s11269-012-0026-0

Avelino, J., Cristancho, M., Georgiou, S., Imbach, P., Aguilar, L., Bornemann, G., Läderach, P., Anzueto, F., Hruska, A.J., Morales, C., 2015. The coffee rust crises in Colombia and Central America (2008–2013): impacts, plausible causes and proposed solutions. Food Sec. 7, 303–321. https://doi.org/10.1007/s12571-015-0446-9

Awange, J.L., Mpelasoka, F., Goncalves, R.M., 2016. When every drop counts: Analysis of Droughts in Brazil for the 1901-2013 period. Science of The Total Environment 566–567, 1472–1488. https://doi.org/10.1016/j.scitotenv.2016.06.031

Beck, H.E., Zimmermann, N.E., McVicar, T.R., Vergopolan, N., Berg, A., Wood, E.F., 2018. Present and future Köppen-Geiger climate classification maps at 1-km resolution. Sci Data 5, 180214. https://doi.org/10.1038/sdata.2018.214

Blain, G.C., 2012. Revisiting the probabilistic definition of drought: strengths, limitations and an agrometeorological adaptation. Bragantia 71, 132–141. https://doi.org/10.1590/S0006-87052012000100019

Blain, G.C., de Avila, A.M.H., Pereira, V.R., 2018. Using the normality assumption to calculate probability-based standardized drought indices: selection criteria with emphases on typical events: USING THE NORMALITY ASSUMPTION TO CALCULATE STANDARDIZED INDICES. Int. J. Climatol 38, e418–e436. https://doi.org/10.1002/joc.5381

Blain, G.C., Meschiatti, M.C., 2015. Inadequacy of the Gamma distribution to calculate the Standardized Precipitation Index. Rev. bras. eng. agríc. ambient. 19, 1129–1135. https://doi.org/10.1590/1807-1929/agriambi.v19n12p1129-1135

Bouroncle, C., Imbach, P., Rodríguez-Sánchez, B., Medellín, C., Martinez-Valle, A., Läderach, P., 2017. Mapping climate change adaptive capacity and vulnerability of smallholder agricultural livelihoods in Central America: ranking and descriptive approaches to support adaptation strategies. Climatic Change 141, 123–137. https://doi.org/10.1007/s10584-016-1792-0

Bundschuh, J., Winograd, M., Day, M., Alvarado, G.E., 2007. Geographical, social, economic, and environmental framework and developments, in: Bundschuh, J., Alvarado, G.E. (Eds.), Central America: Geology, Resources and Hazards. Taylor & Francis, London, pp. 1–52.

Bunn, C., Läderach, P., Ovalle Rivera, O., Kirschke, D., 2015. A bitter cup: climate change profile of global production of Arabica and Robusta coffee. Climatic Change 129, 89–101. https://doi.org/10.1007/s10584-014-1306-x

Burnham, K.P., Anderson, D.R., 2004. Multimodel Inference: Understanding AIC and BIC in Model Selection. Sociological Methods & Research 33, 261–304. https://doi.org/10.1177/0049124104268644

Brenes Torres, A., 2010. Elementos y patrones constitutivos del riesgo de sequía en América Central. Background paper prepared for the 2011 Global Assessment Report on Disaster Risk Reduction. Geneva, Switzerland: UNISDR.

Chen, C.F., Son, N.T., Chen, C.R., Chiang, S.H., Chang, L.Y., Valdez, M., 2017. Drought monitoring in cultivated areas of Central America using multi-temporal MODIS data. Geomatics, Natural Hazards and Risk 8, 402–417. https://doi.org/10.1080/19475705.2016.1222313

Choi, M., Jacobs, J.M., Anderson, M.C., Bosch, D.D., 2013. Evaluation of drought indices via remotely sensed data with hydrological variables. Journal of Hydrology 476, 265–273. https://doi.org/10.1016/j.jhydrol.2012.10.042

Clawson, D.L., 2012. Latin America & the Caribbean: lands and peoples, 5th ed. ed. Oxford University Press, New York.

Crausbay, S.D., Ramirez, A.R., Carter, S.L., Cross, M.S., Hall, K.R., Bathke, D.J., Betancourt, J.L., Colt, S., Cravens, A.E., Dalton, M.S., Dunham, J.B., Hay, L.E., Hayes, M.J., McEvoy, J., McNutt, C.A., Moritz, M.A., Nislow, K.H., Raheem, N., Sanford, T., 2017. Defining Ecological Drought for the Twenty-First Century. Bulletin of the American Meteorological Society 98, 2543–2550. https://doi.org/10.1175/BAMS-D-16-0292.1

Diego Galván, J., Büntgen, U., Ginzler, C., Grudd, H., Gutiérrez, E., Labuhn, I., Julio Camarero, J., 2015. Drought-induced weakening of growth–temperature associations in high-elevation Iberian pines. Global and Planetary Change 124, 95–106. https://doi.org/10.1016/j.gloplacha.2014.11.011

Diffenbaugh, N.S., Swain, D.L., Touma, D., 2015. Anthropogenic warming has increased drought risk in California. Proc Natl Acad Sci USA 112, 3931–3936. https://doi.org/10.1073/pnas.1422385112

Espíndola, E., United Nations, Economic Commission for Latin America and the Caribbean, 2005. Poverty, hunger and food security in Central America and Panama. Naciones Unidas, CEPAL, Social Development Division, Santiago de Chile.

FAO, 2012. FAOSTAT. In: FAOSTAT

Essenwanger, O.M., Landsberg, H.E., Essenwanger, O.M., 2001. Classification of climates, World survey of climatology General climatology. Elsevier, Amsterdam.

Funk, C., Peterson, P., Landsfeld, M., Pedreros, D., Verdin, J., Shukla, S., Husak, G., Rowland, J., Harrison, L., Hoell, A., Michaelsen, J., 2015. The climate hazards infrared precipitation with stations—a new environmental record for monitoring extremes. Sci Data 2, 150066. https://doi.org/10.1038/sdata.2015.66

Gourdji, S., Läderach, P., Valle, A.M., Martinez, C.Z., Lobell, D.B., 2015. Historical climate trends, deforestation, and maize and bean yields in Nicaragua. Agricultural and Forest Meteorology 200, 270–281. https://doi.org/10.1016/j.agrformet.2014.10.002

Gudmundsson L, Stagge, JH., 2014. SCI: Standardized Climate Indices such as SPI, SRI or SPEI. R package version 1.0-1.

Guenang, G.M., Komkoua, M.A.J., Pokam, M.W., Tanessong, R.S., Tchakoutio, S.A., Vondou, A., Tamoffo, A.T., Djiotang, L., Yepdo, Z., Mkankam, K.F., 2019. Sensitivity of SPI to Distribution Functions and Correlation Between its Values at Different Time Scales in Central Africa. Earth Syst Environ 3, 203–214. https://doi.org/10.1007/s41748-019-00102-3

Guttman, N.B., 1999. ACCEPTING THE STANDARDIZED PRECIPITATION INDEX: A CALCULATION ALGORITHM 1. JAWRA Journal of the American Water Resources Association 35, 311–322. https://doi.org/10.1111/j.1752-1688.1999.tb03592.x

Hastenrath, S.L., 1967. Rainfall distribution and regime in Central America. Arch. Met. Geoph. Biokl. B. 15, 201–241. https://doi.org/10.1007/BF02243853

Hayes, M., Svoboda, M., Wall, N., Widhalm, M., 2011. The Lincoln Declaration on Drought Indices: Universal Meteorological Drought Index Recommended. Bulletin of the American Meteorological Society 92, 485–488. https://doi.org/10.1175/2010BAMS3103.1

Heim, R.R., Brewer, M.J., 2012. The Global Drought Monitor Portal: The Foundation for a Global Drought Information System. Earth Interactions 16, 1–28. https://doi.org/10.1175/2012EI000446.1

Imbach, P., Beardsley, M., Bouroncle, C., Medellin, C., Läderach, P., Hidalgo, H., Alfaro, E., Van Etten, J., Allan, R., Hemming, D., Stone, R., Hannah, L., Donatti, C.I., 2017. Climate change, ecosystems and smallholder agriculture in Central America: an introduction to the special issue. Climatic Change 141, 1–12. https://doi.org/10.1007/s10584-017-1920-5

Imbach, P., Chou, S.C., Lyra, A., Rodrigues, D., Rodriguez, D., Latinovic, D., Siqueira, G., Silva, A., Garofolo, L., Georgiou, S., 2018. Future climate change scenarios in Central America at high spatial resolution. PLoS ONE 13, e0193570. https://doi.org/10.1371/journal.pone.0193570

Keyantash, J., Dracup, J.A., 2002. The Quantification of Drought: An Evaluation of Drought Indices. Bull. Amer. Meteor. Soc. 83, 1167–1180. https://doi.org/10.1175/1520-0477-83.8.1167

Köppen, W., 1936. Das geographische System der Klimate, 1–44 (Gebrüder Borntraeger: Berlin, Germany).

Kreft S, Eckstein D, Melchior I., 2016. Global climate risk index 2017: Who suffers most from Extreme weather events? Weather-related loss events in 2014 and 1995 to 2014.

Kriticos, D.J., Webber, B.L., Leriche, A., Ota, N., Macadam, I., Bathols, J., Scott, J.K., 2012. CliMond: global high-resolution historical and future scenario climate surfaces for bioclimatic modelling: CliMond: climate surfaces for bioclimatic modelling. Methods in Ecology and Evolution 3, 53–64. https://doi.org/10.1111/j.2041-210X.2011.00134.x

Krozer, A., 2010. A regional basic income: towards the eradication of extreme poverty in Central America. ECLACL Working Paper LC/MEX/L.998

Läderach, P., Ramirez–Villegas, J., Navarro-Racines, C., Zelaya, C., Martinez–Valle, A., Jarvis, A., 2017. Climate change adaptation of coffee production in space and time. Climatic Change 141, 47–62. https://doi.org/10.1007/s10584-016-1788-9

Liu, Y., Zhu, Y., Ren, L., Yong, B., Singh, V.P., Yuan, F., Jiang, S., Yang, X., 2019. On the mechanisms of two composite methods for construction of multivariate drought indices. Science of The Total Environment 647, 981–991. https://doi.org/10.1016/j.scitotenv.2018.07.273

Lloyd-Hughes, B., Saunders, M.A., 2002. A drought climatology for Europe. Int. J. Climatol. 22, 1571–1592. https://doi.org/10.1002/joc.846

Ma, F., Yuan, X., Ye, A., 2015. Seasonal drought predictability and forecast skill over China. J. Geophys. Res. Atmos. 120, 8264–8275. https://doi.org/10.1002/2015JD023185

Magaña, V., Amador, J., Medina, S., 1999. The Midsummer Drought over Mexico and Central America. Journal of Climate - J CLIMATE. 12. 1577-1588. 10.1175/1520-0442(1999)012<1577:TMDOMA>2.0.CO;2.

Maria, A., Acero, J.L., Aguilera, A.I., Lozano, M.G. (Eds.), 2017. Central America Urbanization Review: Making Cities Work for Central America. The World Bank. https://doi.org/10.1596/978-1-4648-0985-9

Marshall, J., 2007. The Geomorphology and Physiographic Provinces of Central America, in: Bundschuh, J., Alvarado, G.E. (Eds.), Central America: Geology, Resources and Hazards. Taylor & Francis, London, pp. 75–122.

Martinson, T.L., 1993. Physical environments of Latin America, in: Blouet, B.W.& O.M. (Ed.), Latin America and the Caribbean: A Systematic and Regional Survey. Wiley, New York, pp. 1–33.

McKee, T.B., Doesken, N.J. and Kleist, J., 1993. The relationship of drought frequency and duration to time scales. In: Proceedings of the Eighth Conference on Applied Climatology. Boston, IL: American Meteorological Society, pp. 179–184.

Meschiatti, M.C., Blain, G.C., 2016. Increasing the regional availability of the Standardized Precipitation Index: an operational approach. Bragantia 75, 507–521. https://doi.org/10.1590/1678-4499.478

Mishra, A.K., Singh, V.P., 2011. Drought modeling – A review. Journal of Hydrology 403, 157–175. https://doi.org/10.1016/j.jhydrol.2011.03.049

Mo, K.C., Lyon, B., 2015. Global Meteorological Drought Prediction Using the North American Multi-Model Ensemble. Journal of Hydrometeorology 16, 1409–1424. https://doi.org/10.1175/JHM-D-14-0192.1

Mosiño AP, García E., 1966. Evaluación de la sequía intraestival en la República Mexicana. Proc. Conf. Reg. Latinoamericana Unión Geogr. Int. 1966; 3: 500–516.

Nakaegawa, T., Kitoh, A., Murakami, H., Kusunoki, S., 2014. Annual maximum 5-day rainfall total and maximum number of consecutive dry days over Central America and the Caribbean in the late twenty-first century projected by an atmospheric general circulation model with three different horizontal resolutions. Theor Appl Climatol 116, 155–168. https://doi.org/10.1007/s00704-013-0934-9

Naresh Kumar, M., Murthy, C.S., Sesha Sai, M.V.R., Roy, P.S., 2009. On the use of Standardized Precipitation Index (SPI) for drought intensity assessment. Met. Apps 16, 381–389. https://doi.org/10.1002/met.136

Peel, M.C., Finlayson, B.L., McMahon, T.A., 2007. Updated world map of the Köppen-Geiger climate classification. Hydrol. Earth Syst. Sci. 11, 1633–1644. https://doi.org/10.5194/hess-11-1633-2007

Pieper, P., Düsterhus, A., Baehr, J., 2020. Global and regional performances of SPI candidate distributionfunctions in observations and simulations (preprint). Hydrometeorology/Theory development. https://doi.org/10.5194/hess-2019-614

Quesada-Montano, B., Wetterhall, F., Westerberg, I.K., Hidalgo, H.G., Halldin, S., 2019. Characterising droughts in Central America with uncertain hydro-meteorological data. Theor Appl Climatol 137, 2125–2138. https://doi.org/10.1007/s00704-018-2730-z

Ramirez P. and Brenes A., 2001. Condiciones de sequia observadas en el Istmo Centroamericano en el ano 2001. Documento Técnico, Comité Regional de Recursos Hidraulicos (CRRH), Sistema de Integracion Centroamericano (SICA), San José, Costa Rica.

Russell, R. J., 1931. Dry climates of the United States: I climatic map, vol. 5 of Publications in Geography. (University of California)

Seier, E., 2011. Normality Tests: Power Comparison, in: Lovric, M. (Ed.), International Encyclopedia of Statistical Science. Springer Berlin Heidelberg, Berlin, Heidelberg, pp. 1000–1003. https://doi.org/10.1007/978-3-642-04898-2_421

Shapiro, S.S., Wilk, M.B., 1965. An Analysis of Variance Test for Normality (Complete Samples). Biometrika 52, 591. https://doi.org/10.2307/2333709

Sienz, F., Bothe, O., Fraedrich, K., 2012. Monitoring and quantifying future climate projections of dryness and wetness extremes: SPI bias. Hydrol. Earth Syst. Sci. 16, 2143–2157. https://doi.org/10.5194/hess-16-2143-2012

Stagge, J.H., Tallaksen, L.M., Gudmundsson, L., Van Loon, A.F., Stahl, K., 2015. Candidate Distributions for Climatological Drought Indices (SPI and SPEI): CANDIDATE DISTRIBUTIONS FOR CLIMATOLOGICAL DROUGHT INDICES. Int. J. Climatol. 35, 4027–4040. https://doi.org/10.1002/joc.4267

Stephens, M.A., 1974. EDF Statistics for Goodness of Fit and Some Comparisons. Journal of the American Statistical Association 69, 730–737. https://doi.org/10.1080/01621459.1974.10480196

Taylor, M.A., Alfaro, E.J., 2005. Central America and the Caribbean, Climate of, in: Oliver, J.E. (Ed.), Encyclopedia of World Climatology, Encyclopedia of Earth Sciences Series. Springer Netherlands, pp. 183–189. https://doi.org/10.1007/1-4020-3266-8_37

Touma, D., Ashfaq, M., Nayak, M.A., Kao, S.-C., Diffenbaugh, N.S., 2015. A multi-model and multi-index evaluation of drought characteristics in the 21st century. Journal of Hydrology 526, 196–207. https://doi.org/10.1016/j.jhydrol.2014.12.011

Trenberth, K.E., Dai, A., van der Schrier, G., Jones, P.D., Barichivich, J., Briffa, K.R., Sheffield, J., 2014. Global warming and changes in drought. Nature Clim Change 4, 17–22. https://doi.org/10.1038/nclimate2067

United Nations, 2019. Department of Economic and Social Affairs, Population Division . World Population Prospects 2019: Volume II: Demographic Profiles.

van Oldenborgh G, Collins M, Arblaster J, Christensen J, Marotzke J, Power S, et al., 2013. IPCC. Annex I: Atlas of Global and Regional Climate Projections. In Stocker T. F., Qin D., Plattner G.-K., Tignor M., Allen S. K., Boschung J., … Midgley P. M. (Eds.), Climate Change 2013: The Physical Science Basis. Contribution of Working Group I to the Fifth Assessment Report of the Intergovernmental Panel on Climate Change (pp. 1311–1394). Cambridge, United Kingdom and New York, NY, USA: Cambridge University Press; 2013.

Vicente-Serrano, S.M., Beguería, S., López-Moreno, J.I., 2010. A Multiscalar Drought Index Sensitive to Global Warming: The Standardized Precipitation Evapotranspiration Index. Journal of Climate 23, 1696–1718. https://doi.org/10.1175/2009JCLI2909.1

Wilhite, D.A. (Ed.), 2000. Drought: a global assessment, Routledge hazards and disasters series. Routledge, London ; New York.

Wu, H., Svoboda, M.D., Hayes, M.J., Wilhite, D.A., Wen, F., 2007. Appropriate application of the standardized precipitation index in arid locations and dry seasons. Int. J. Climatol. 27, 65–79. https://doi.org/10.1002/joc.1371

Yoon, J.-H., Mo, K., Wood, E.F., 2012. Dynamic-Model-Based Seasonal Prediction of Meteorological Drought over the Contiguous United States. Journal of Hydrometeorology 13, 463–482. https://doi.org/10.1175/JHM-D-11-038.1

Yuan, X., Wood, E.F., 2013. Multimodel seasonal forecasting of global drought onset. Geophys. Res. Lett. 40, 4900–4905. https://doi.org/10.1002/grl.50949

VIII Ehrenwörtliche Erklärung

Hiermit erkläre ich, dass die Arbeit selbständig und nur unter Verwendung der angegebenen Hilfsmittel angefertigt wurde.

Freiburg, 28.10.2020 Anneke Ewert

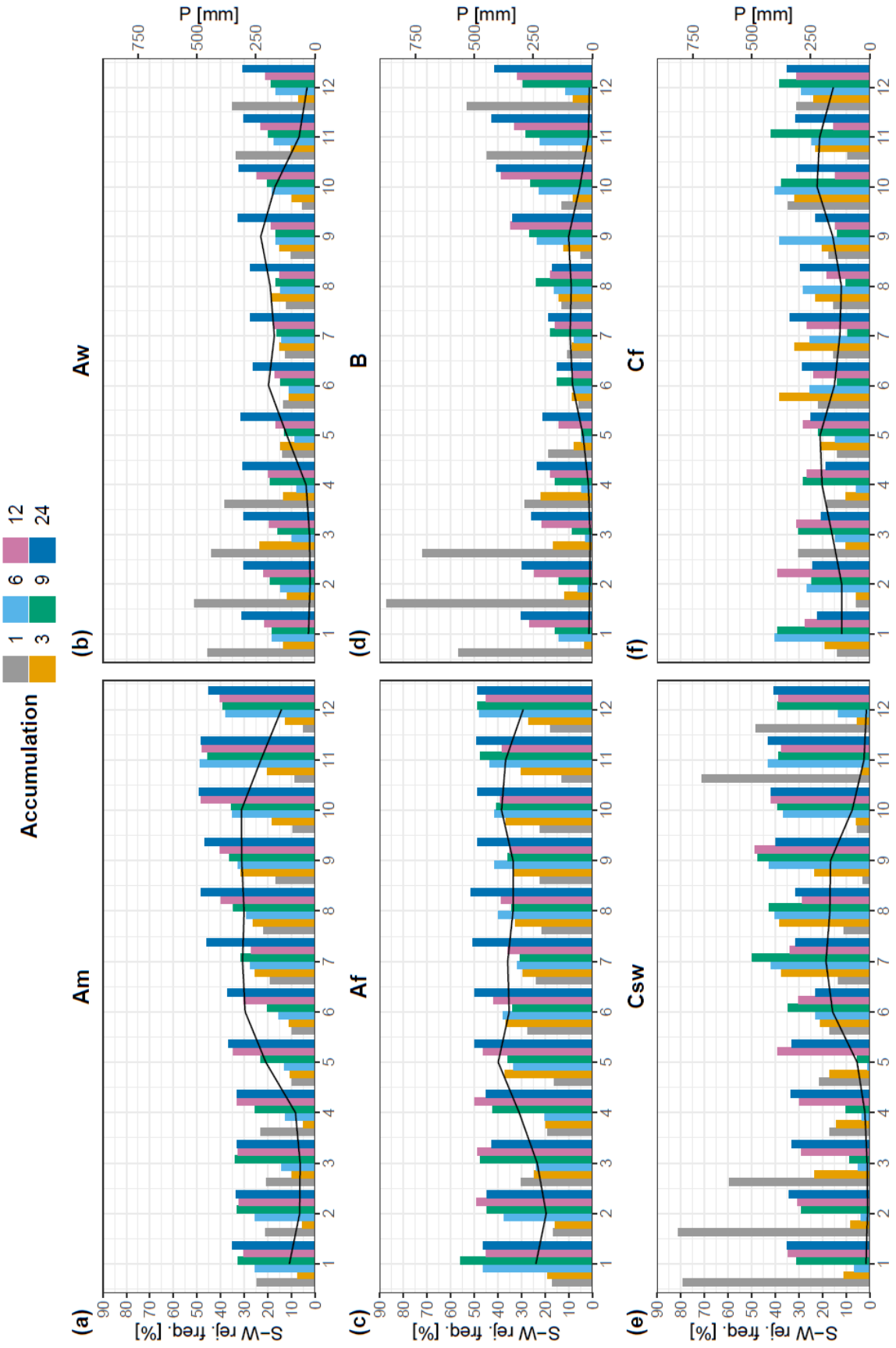

Figure S 1: Rejection frequency [%] of the S-W test of the Gumbel distribution per accumulation period during the year and the mean annual precipitation for the climate zones Am, Aw, Af, B, Csw and Cf

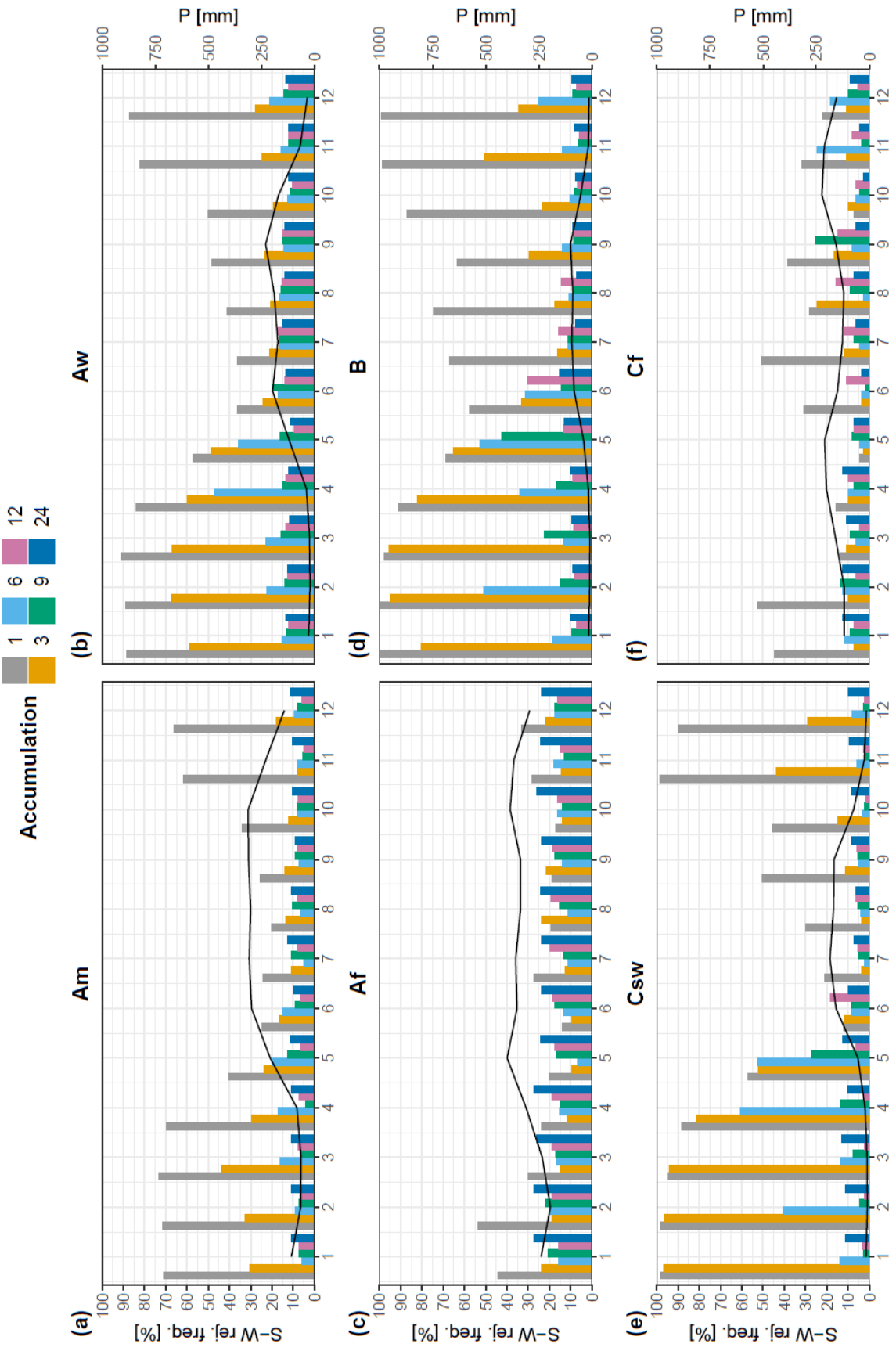

Figure S 2: Rejection frequency [%] of the S-W test of the Normal distribution per accumulation period during the year and the mean annual precipitation for the climate zones Am, Aw, Af, B, Csw and Cf

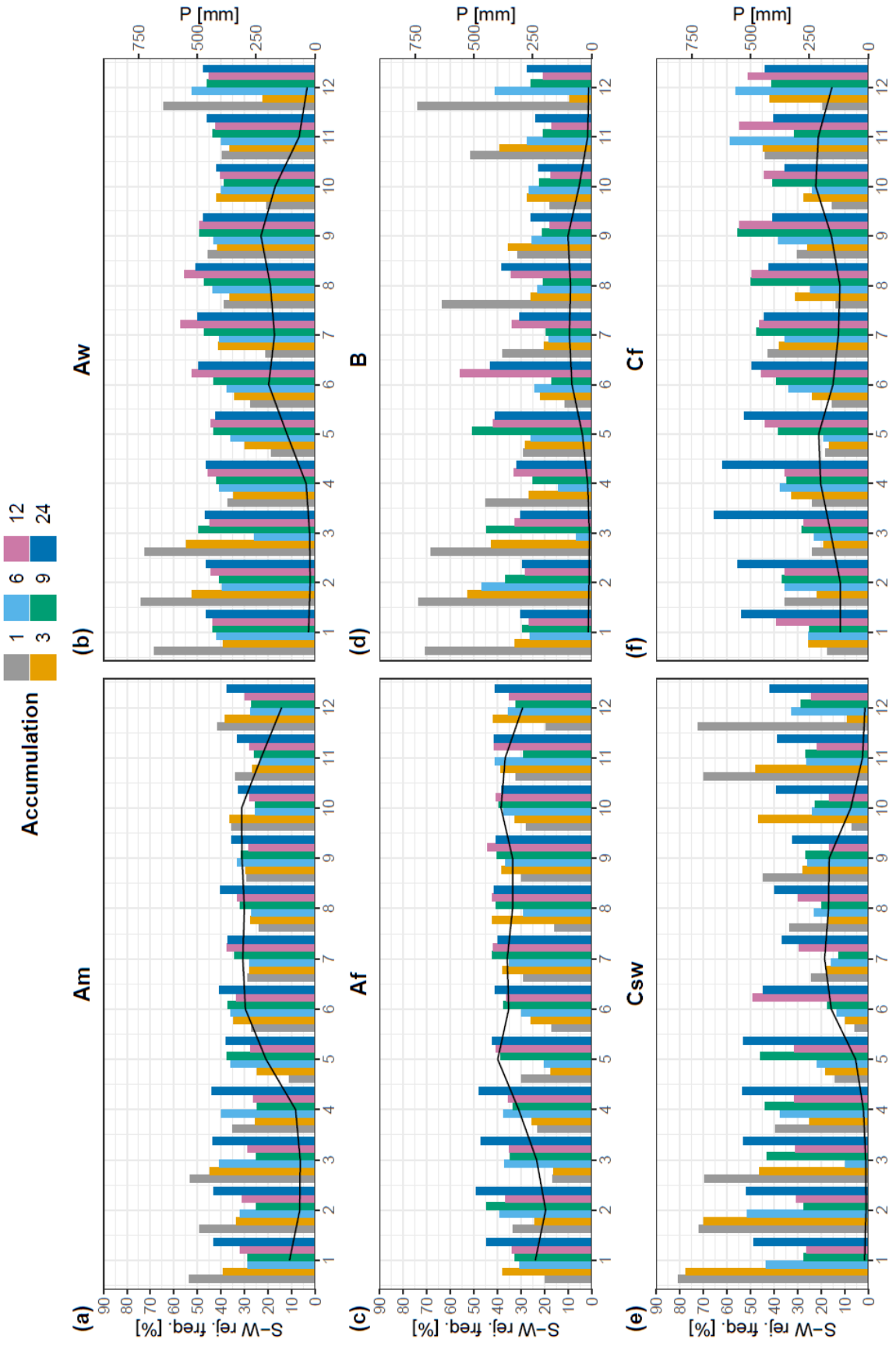

Figure S 3: Rejection frequency [%] of the S-W test of the Weibull distribution per accumulation period during the year and the mean annual precipitation for the climate zones Am, Aw, Af, B, Csw and Cf

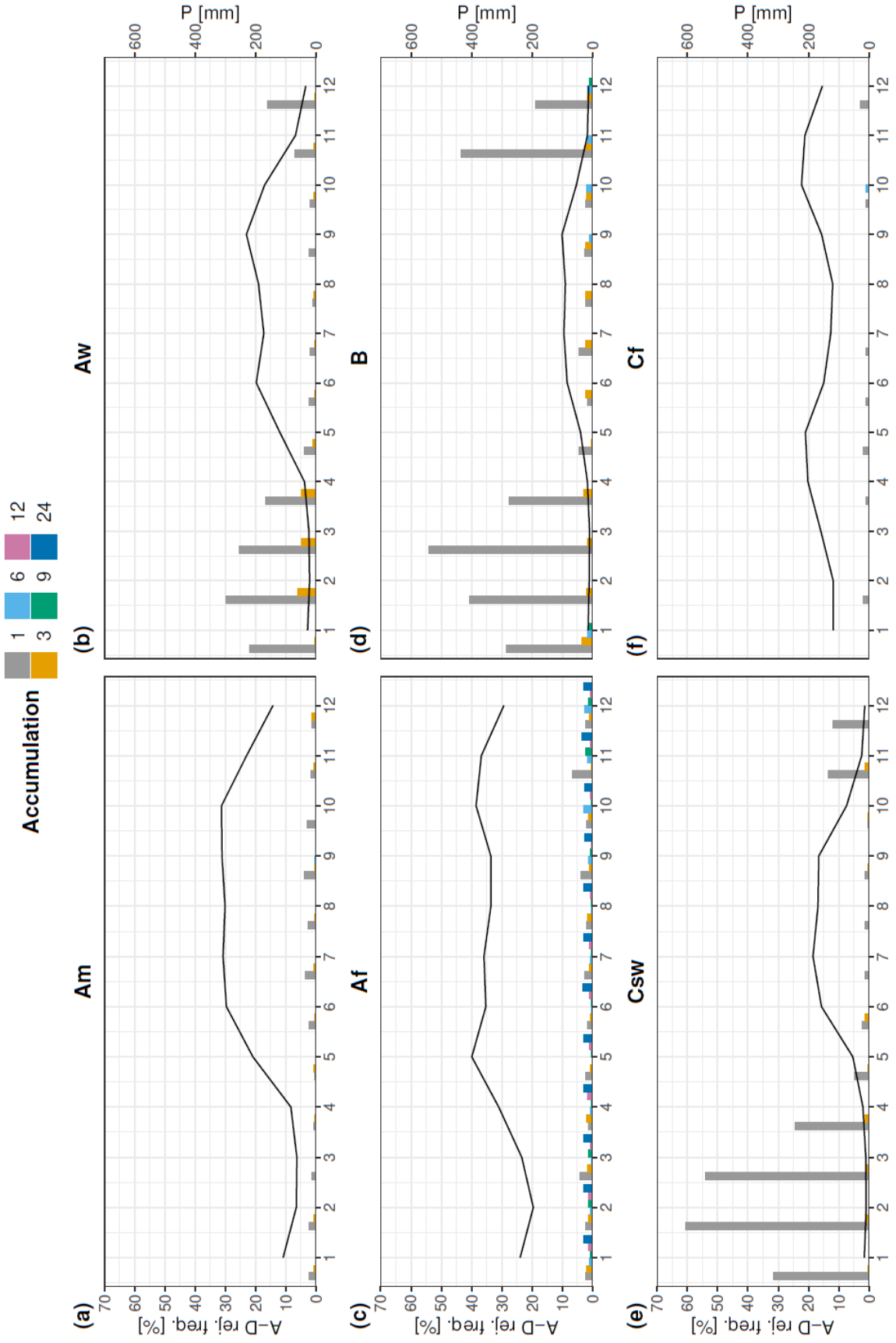

Figure S 4: Rejection frequency [%] of the A-D test of the Gamma distribution per accumulation period during the year and the mean annual precipitation for the climate zones Am, Aw, Af, B, Csw and Cf

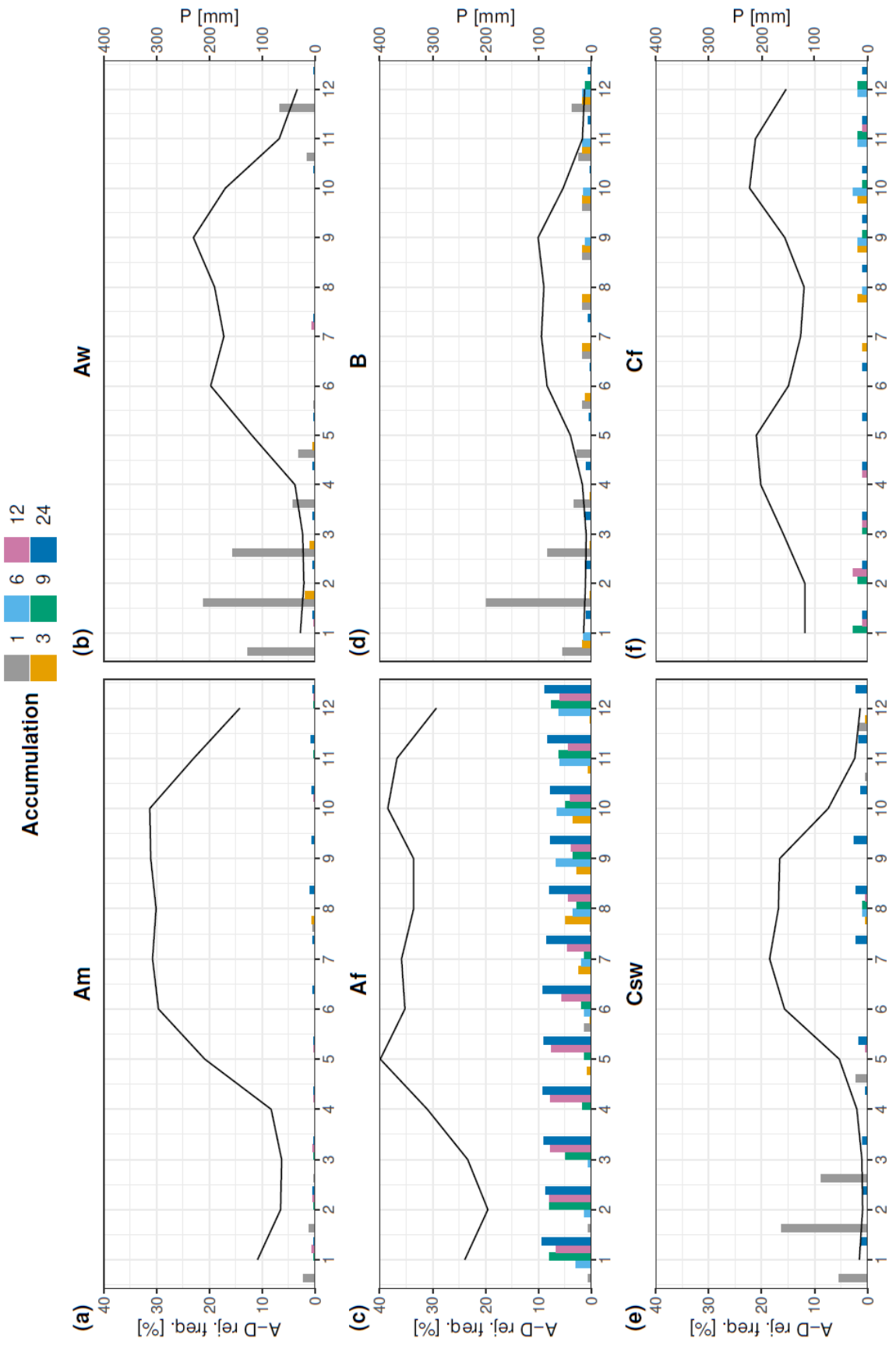

Figure S 5: Rejection frequency [%] of the A-D test of the Gumbel distribution per accumulation period during the year and the mean annual precipitation for the climate zones Am, Aw, Af, B, Csw and Cf

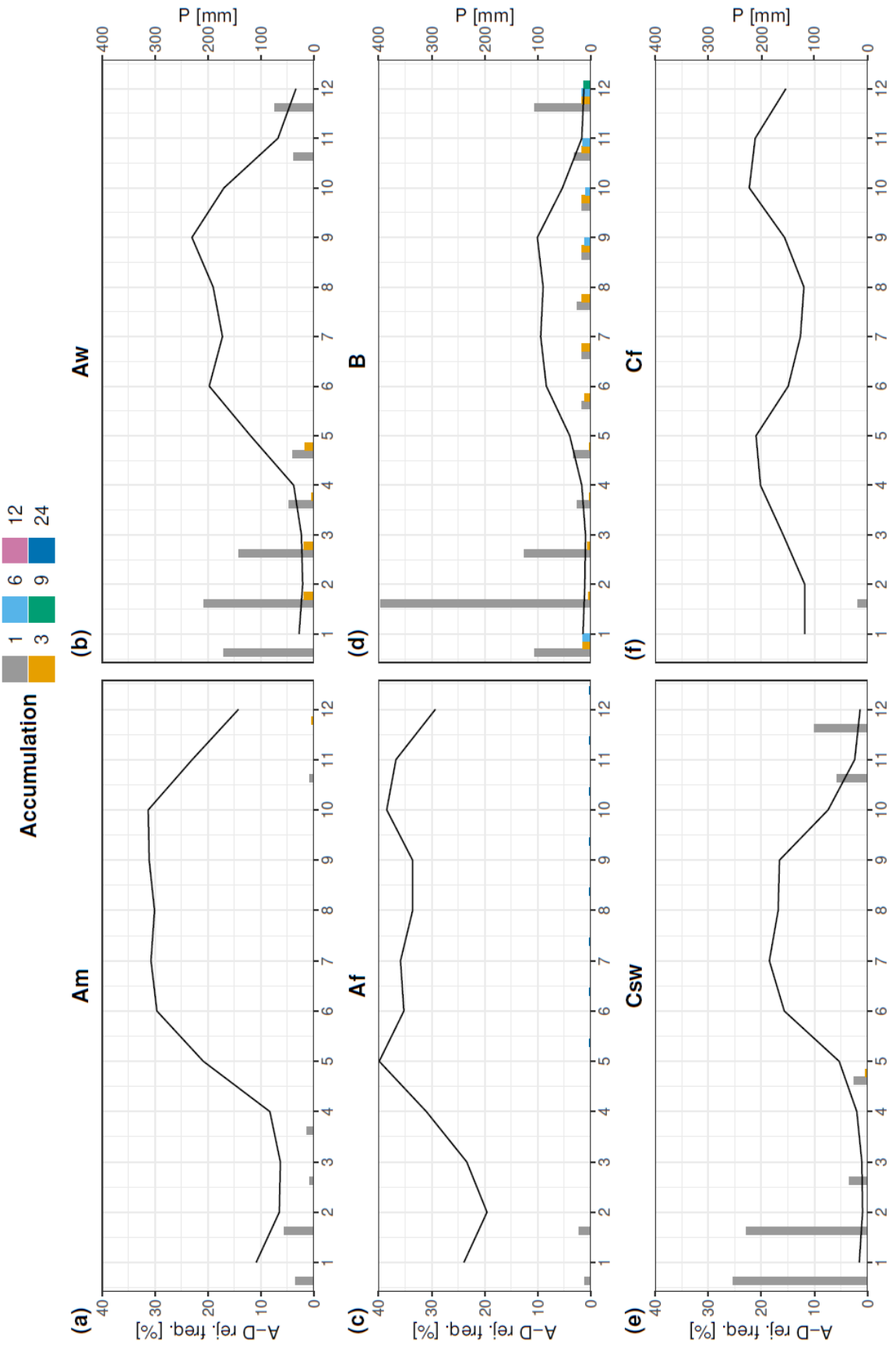

Figure S 6: Rejection frequency [%] of the A-D test of the Logistic distribution per accumulation period during the year and the mean annual precipitation for the climate zones Am, Aw, Af, B, Csw and Cf

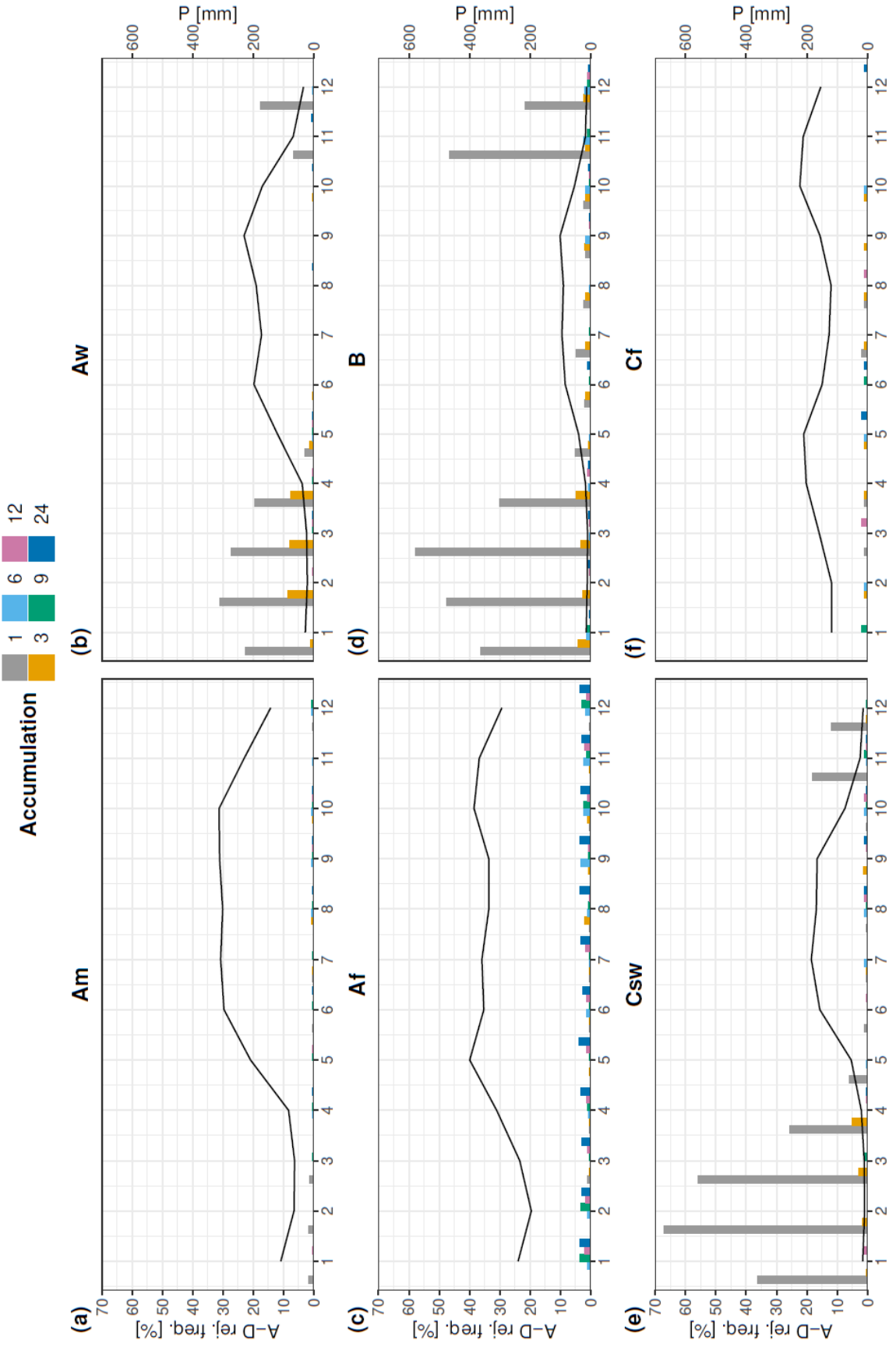

Figure S 7: Rejection frequency [%] of the A-D test of the Lognormal distribution per accumulation period during the year and the mean annual precipitation for the climate zones Am, Aw, Af, B, Csw and Cf

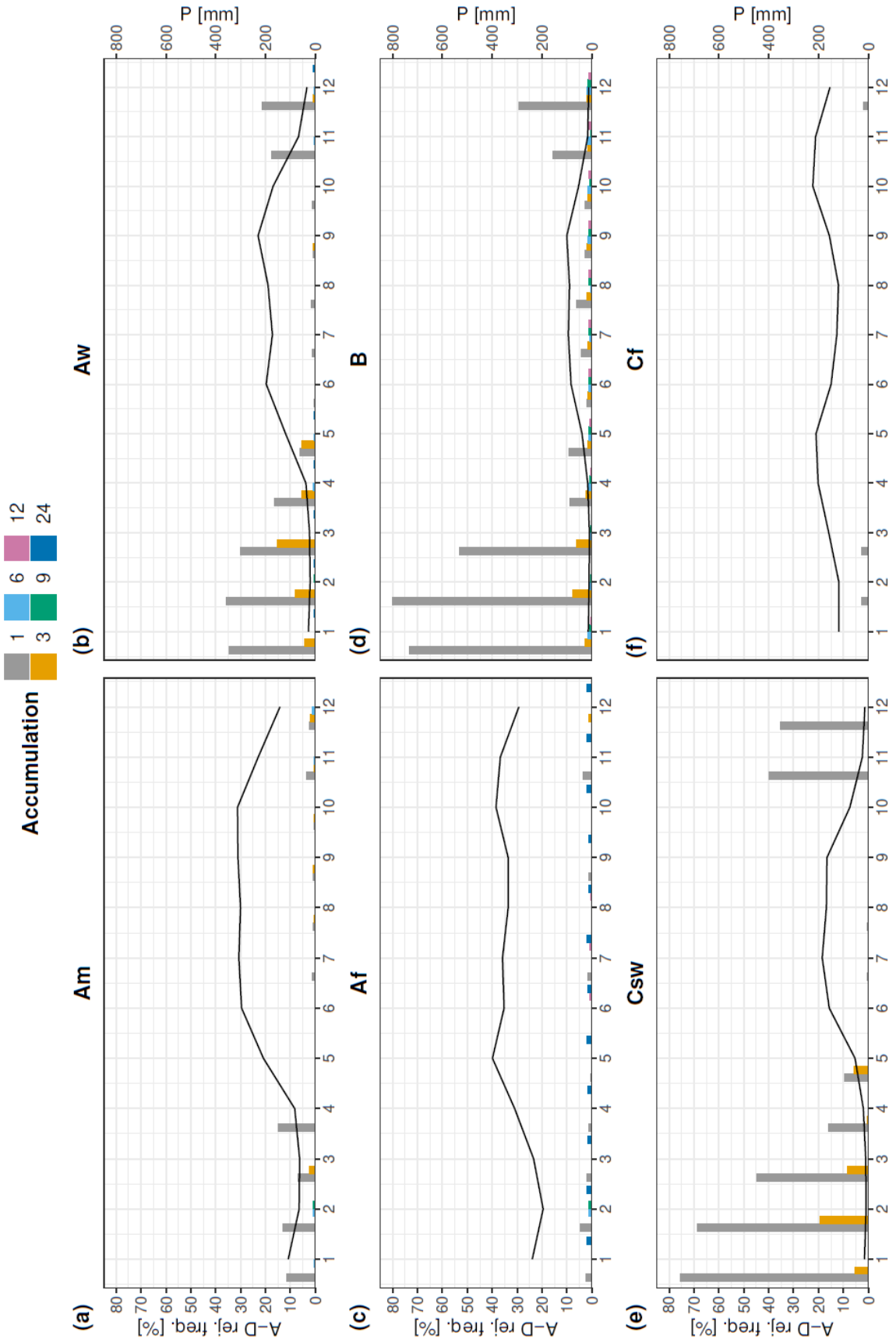

Figure S 8: Rejection frequency [%] of the A-D test of the Normal distribution per accumulation period during the year and the mean annual precipitation for the climate zones Am, Aw, Af, B, Csw and Cf

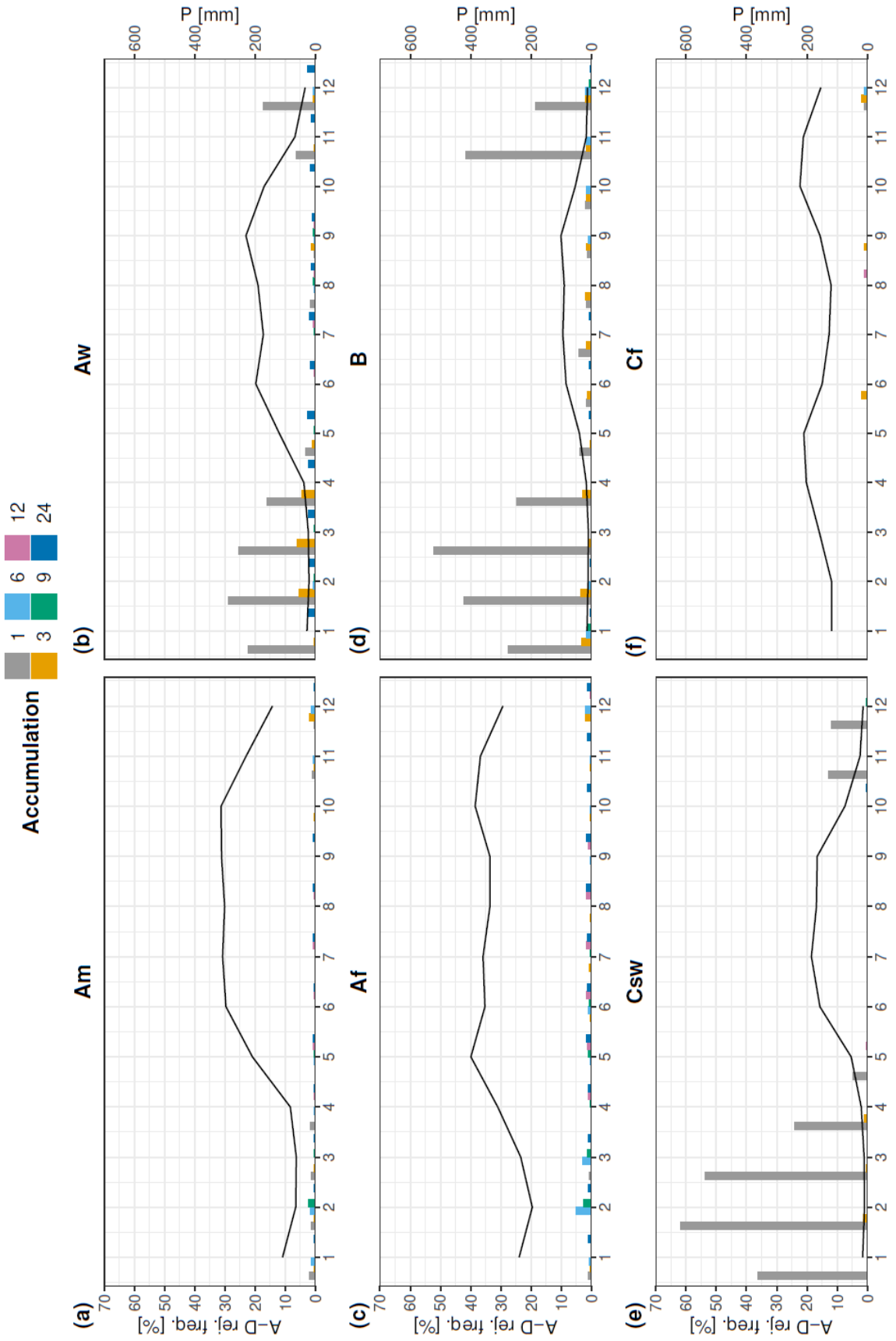

Figure S 9: **Rejection frequency [%] of the A-D test of the Weibull distribution per accumulation period during the year and the mean annual precipitation for the climate zones Am, Aw, Af, B, Csw and Cf**